agriculture

MDPI

Article

Modelling the Hydrology of an Upland Catchment of Bystra River in 2050 Climate Using RCP 4.5 and RCP 8.5 Emission Scenario Forecasts

Damian Badora *, Rafal Wawer, Anna Nierobca, Aleksandra Krol-Badziak, Jerzy Kozyra, Beata Jurga and Eugeniusz Nowocien

The Institute of Soil Science and Plant Cultivation—State Research Institute, ul. Czartoryskich 8, 24-100 Pulawy, Poland; huwer@iung.pulawy.pl (R.W.); anna.nierobca@iung.pulawy.pl (A.N.); aleksandra.krol@iung.pulawy.pl (A.K.-B.); kozyr@iung.pulawy.pl (J.K.); bjurga@iung.pulawy.pl (B.J.); nowocien@iung.pulawy.pl (E.N.)

* Correspondence: dbadora@iung.pulawy.pl

Abstract: This article presents selected flow modeling indices of the Bystra River catchment area (east Poland) obtained using the SWAT model simulations for three regional climate models driven by the EC-EARTH global climate model for 2021–2050 and both RCP4.5 and RCP 8.5 scenarios. The research area was selected due to the large relief of the terrain, the predominance of soils made of loess and the agricultural nature of the Bystra River catchment area, which is very sensitive to climate change, has very valuable soils, and can be used as a test area for modeling land use-based adaptation measures to climate change. The calibration and validation using the SUFI-2 algorithm in the SWAT CUP program was carried out in order to determine the water balance. After obtaining satisfactory results, the SWAT-CUP program simulated the best parameter values for climate change projections. In analyzed climate projections, the monthly mean sums of actual evapotranspiration and potential evapotranspiration will be higher compared to the simulation period of the 2010–2017 model. The exception is the month of June, where actual evapotranspiration in most climate projections is lower compared to the years 2010–2017. The average monthly total runoff for the Bystra River basin will be lower in most of the 2021–2030 climate change projections for most months compared to the reference period. Also, in the 2031–2040 and 2041–2050 periods, the average monthly total runoff will be lower for the RCP 4.5 scenarios (except for one RCP 4.5 scenario in 2031–2040). Additionally, in the case of the RCP 8.5 for the two scenarios in 2041–2050, the average monthly total runoff will be higher compared to the reference years. We determine that the analysis impact of climate change will result in 31 recognized and different small sub-catchments of the Bystra River, which result from higher precipitation and less evapotranspiration for RCP 8.5 in 2041–2050. All of the above changes in the individual components of the water balance may have a negative impact on the vegetation in the coming decades. The temperature increase and the variable amount of precipitation in individual months may lead to an increased number of extreme phenomena. Increased mean monthly sum of actual and potential evapotranspiration, as well as changes in monthly sums of total runoff, may disturb the vegetation in the studied area at every stage of growth. The above components may also influence changes in the amount of water in the soil (especially during the growing season). Counteracting the effects of future climate change requires various adaptation measures.

Keywords: climate change; water deficit; SWAT; SWAT-CUP

Citation: Badora, D.; Wawer, R.; Nierobca, A.; Krol-Badziak, A.; Kozyra, J.; Jurga, B.; Nowocien, E. Modelling the Hydrology of an Upland Catchment of Bystra River in 2050 Climate Using RCP 4.5 and RCP 8.5 Emission Scenario Forecasts. *Agriculture* **2022**, *12*, 403. https://doi.org/10.3390/agriculture12030403

Academic Editors: Alban Kuriqi and Luis Garrote

Received: 3 December 2021
Accepted: 4 March 2022
Published: 14 March 2022

1. Introduction

Climate change for the next few decades to come and the related unpredictability of extreme weather phenomena are currently the subject of many studies. This is due to concerns about the environmental, social, and economic risks that may arise in the coming decades. These changes will also apply to agriculture in Poland [1]. The analysis

of the climate for the years 1970–2010 shows a statistically significant increase in the sum of evapotranspiration in the growing season [2]. The increase in evapotranspiration, temperature, and precipitation in the coming decades will also apply to the Vistula basin [3] and Europe as a whole [4,5].

Moreover, the amount of precipitation increases in winter and early spring and decreases in spring and summer. This contributes to the reduction of the climatic water balance (i.e., the increase in the deficit of precipitation in relation to the potential evaporation) [2].

The observed increase in air temperature contributed to the increase in potential evapotranspiration. In particular, in the 2011–2020 period, a large increase in potential evapotranspiration was found and the variability of this indicator increased (Figure 1).

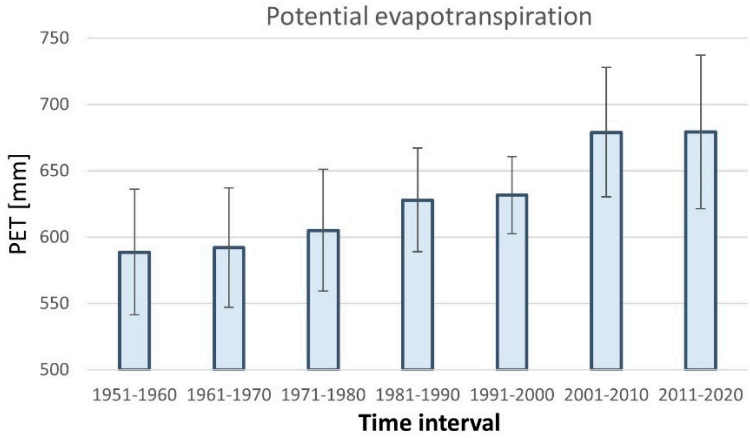

Figure 1. Potential evapotranspiration in Pulawy with error bars calculated according to the Doroszewski formula [6].

In recent decades, changes in the climate have been observed in Poland, resulting from warming, changes in precipitation, and a number of extreme weather events [7–9]. Climate change scenarios developed by the IPCC [10] indicate a 10-fold increase in the occurrence of droughts in Poland in the coming decades [11]. According to NOAA, 2017 was the second warmest year of meteorological recording and analysis (since 1880) in the world [12]. By analyzing the climate scenarios for the years 2021–2050, it has been shown that the growing season in Poland, defined by the number of days with the daily air temperature 5 °C higher in the years 2021–2050, will be longer than in the years 1971–2000 by 16 days. The predicted higher temperature in the growing season of plants will significantly accelerate their development [2]. Therefore, it is necessary to look for solutions to minimize the negative impact of climate change [13], e.g., the occurrence of weather extremes and droughts [6,14–17] in the Bystra catchment areas, in the coming decades. In order to assess the effectiveness of the proposed solutions, it is necessary to develop boundary conditions, indicating a baseline representing the behavior of the Bystra catchment hydrosystem in the 'business as usual scenario' (i.e., taking into account changes in the hydrological cycle caused only by climate change with unchanged conditions of human activity). The above-mentioned boundary conditions for the 2050 horizon must be based on simulation modeling, calibrated on archival data. One of the many mathematical models suitable for the analysis of the water balance of the catchment area and the analysis of the impact of predicted climate changes in the future decades is the SWAT model.

This study uses large scale application SWAT for Vistula and Odra large catchment-based analysis to determine increases of both low and high river flows [18]. It was also shown that soil moisture and soil physical properties add valuable information for the prediction of climate change impact on yield variability [18].

The purpose of this article is to prepare an appropriate SWAT model and to study spatial assessment of hydrological indices obtained in three varied climate projections for two representative concentration pathways (RCPs) in order to analyze differences

in the results of regional climate models based on the same global climate model [19]. These models are characterized by different parameterization of physical processes while running on the same spatial domain, covering the European continent, and benefiting from the boundary and initial conditions of the same global model (EC-EARTH). Such assessment attitudes matter for future research on the effectiveness of agricultural land use change adaptation practices in terms of reducing water erosion and increasing water retention in the landscape, including small retention, introduced in various variants related to land consolidation.

The developed model, after calibration and validation, was used for research related to the prepared projections for the RCP 4.5 and RCP 8.5 scenarios.

The study area was selected due to the large relief and the predominance of soils made of loess. The agricultural nature of the catchment area and loess soils with good retention properties [20] will be used in subsequent publications to assess adaptation scenarios. The Bystra catchment area has been the target of many studies and statutory re-search by IUNG. The results of these studies have been used in this present study.

Due to the observed temperature increase, which also contributes to the increase in potential evapotranspiration in recent years, the years 2010–2017 were adopted for the SWAT model.

The aim of the article is to analyze the hydrology of the Bystra River basin in the 2021–2050 climate projections for the RCP 4.5 and RCP 8.5 climate change scenarios, as well as to provide an assessment against the background of the current state of knowledge related to research covering the European continent and small regional catchments.

2. Study Area

The Bystra River, which is the right tributary of the Vistula River, 33 km long and 306.9 km^2 in area, is located in the Lubelskie Voivodeship (Figure 2). The Bystra River basin is a second order hydrographic unit (Code PLRW2000923899) [21]. According to the generated SWAT model, the lowest point of the catchment area is 123 m above sea level, while the highest point is 246 m above sea level. The catchment area is 296.6 km^2.

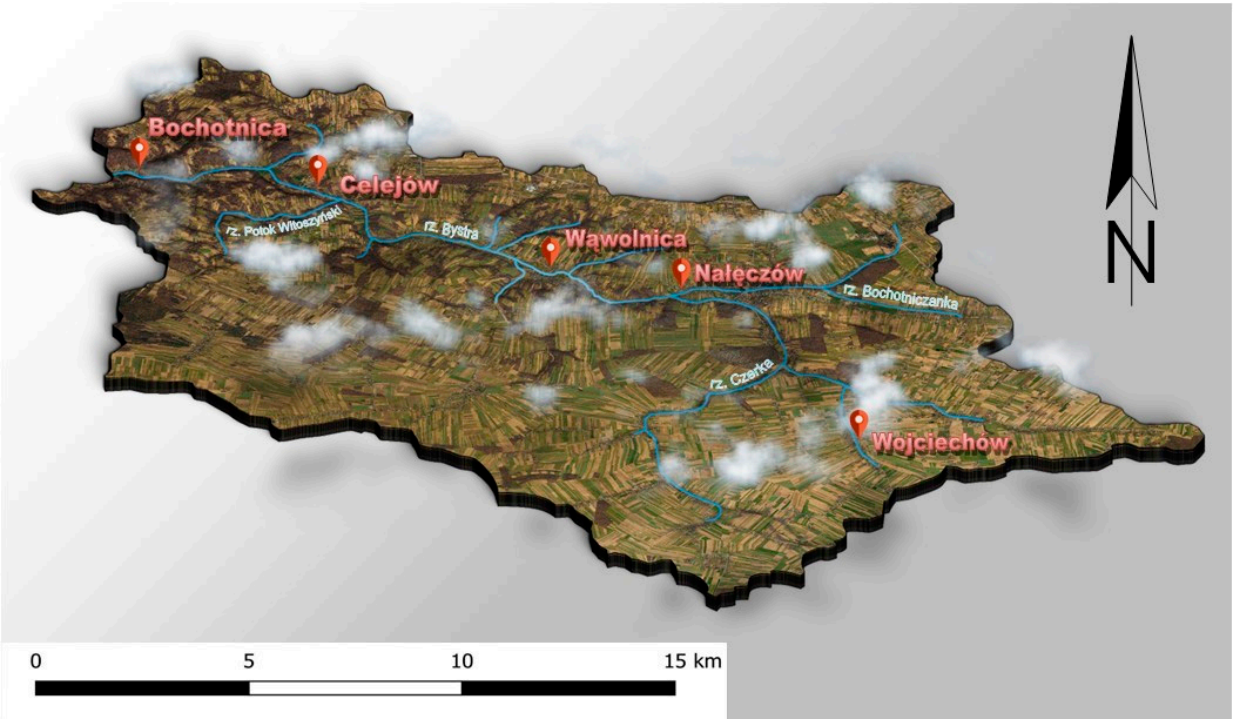

Figure 2. The catchment area of the Bystra River (own study).

The Bystra River basin part of the Lublin Upland [22–24] The relief of the Bystra River valley and its tributaries is very large and consists of many valley forms with a constant or episodic inflow. There are few valleys with a constant tributary. The largest of them, the Bystra valley, is 35 km long. In the section where the Bystra River valley flows into the Vistula, it cuts up to 35 m in marl and rocks [21,25,26].

Virtually the entire catchment area is built of a deep loess (up to 20 m). In the deeper layers there are Quaternary Pleistocene deposits, glacial sands and gravels, and slightly deeper tilts. Paleocene Paleogene deposits lie under the clay (i.e., geoses). On the other hand, under the geezes there are upper Cretaceous deposits (i.e., rocks with limestone inserts) [27].

The upland nature of the catchment area with a predominance of loess soils and the high slopes of the slopes at the mouth of the Bystra River pose a significant threat to the catchment area in terms of medium and very strong water and surface erosion [28].

According to the raster soil map prepared for the SWAT model (Figure 3), the study area consists mainly of podzolic and pseudo-polygonal soils (49%) as well as leached brown soils and acid soils (47%) (Table 1).

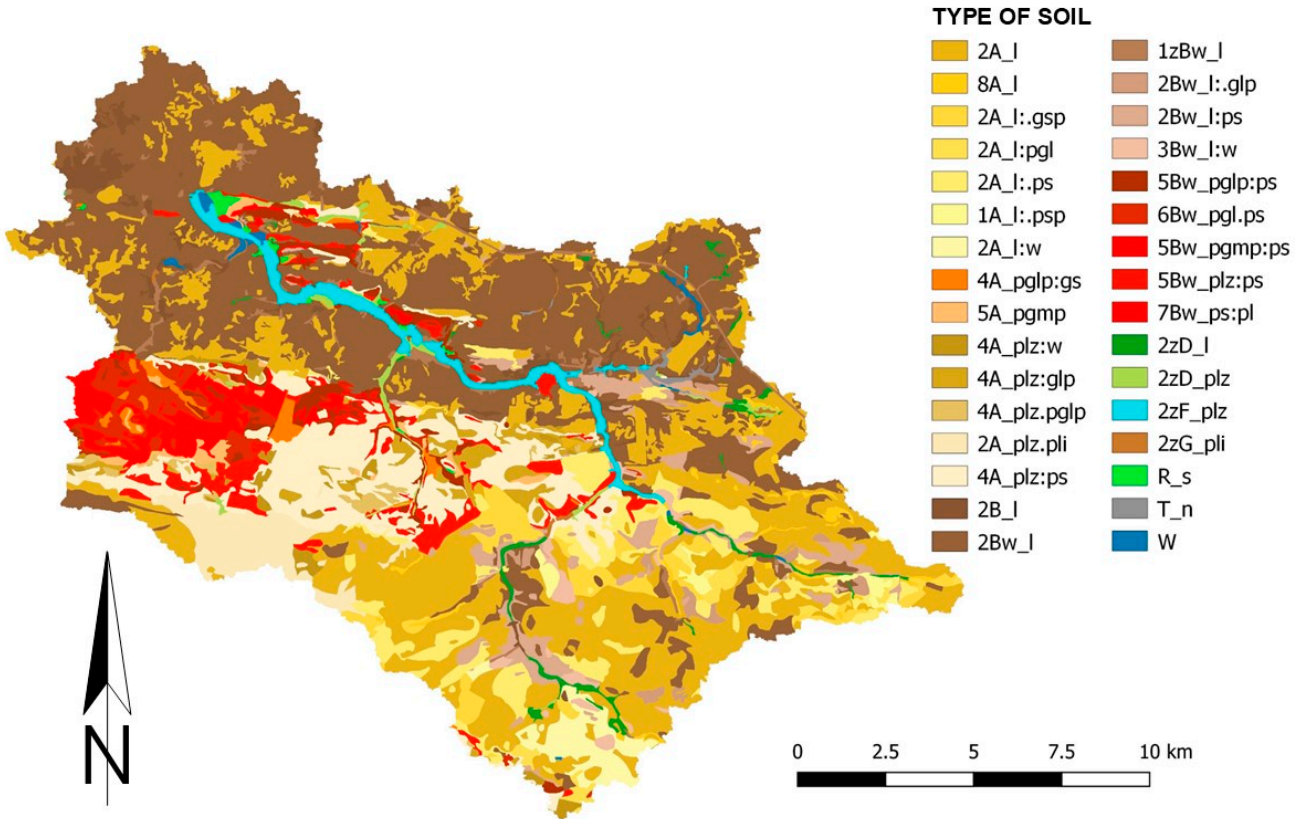

Figure 3. Soil map introduced to the SWAT model with division into soil types (own study).

Overall, 32 grain size groups were separated. Podzolic soils extend mainly in the south-eastern area of the catchment area, while brown soils dominate in the north-west area. Loess (73%) [29–31] and ordinary dust (18%) dominate in the soil cover of the Bystra River catchment area.

According to the map of the cover and land use of the Bystra River catchment area, arable lands (78%) and forests (16%) dominate (Figure 4).

Table 1. Division into soil types and species and the percentage share of soils in the Bystra basin gener-ated in the QSWAT interface (own study).

Soil Agricultural Complex	Type of Soil	Type of Fraction	[%] Part	Soil Agricultural Complex	Type of Soil	Type of Fraction	[%] Part
2	**A**	l	24.8	5	**Bw**	plz:ps	2.7
4	**A**	plz:ps	7.6	7	**Bw**	ps	2.1
2	**A**	l:.ps	4.7	6	**Bw**	pgl.ps	2.0
2	**A**	l:.gsp	2.5	5	**Bw**	pglp:ps	1.8
2	**A**	plz.pli	2.5	1z	**Bw**	l	1.3
4	**A**	plz:glp	1.5	3	**Bw**	l:w	0.7
2	**A**	l:w	1.5	2	**Bw**	l:.glp	0.7
4	**A**	plz	0.9	5	**Bw**	pgmp:ps	0.7
8	**A**	l	0.7	2	**B**	l	1.9
4	**A**	pglp:gs	0.7	2z	**F**	plz	1.7
5	**A**	pgmp	0.6	2z	**D**	l	0.8
2	**A**	l:pgl	0.6	2z	**D**	plz	0.7
1	**A**	l:.psp	0.6	-	**W**		0.3
4	**A**	plz.pglp	0.5	-	**R**	s	0.2
2	**Bw**	l	30.2	-	**T**	n	0.2
2	**Bw**	l:ps	2.9	2z	**G**	pli	0.1
[%] Share of Haplic Podzols and Albic Luvisol soils (A)							49
[%] Share of Haplic Cambisol, Brunic Arenosols and Haplic Cambisol Eutric soils (Bw)							47
[%] Share of loess							73
[%] Share of silt							18

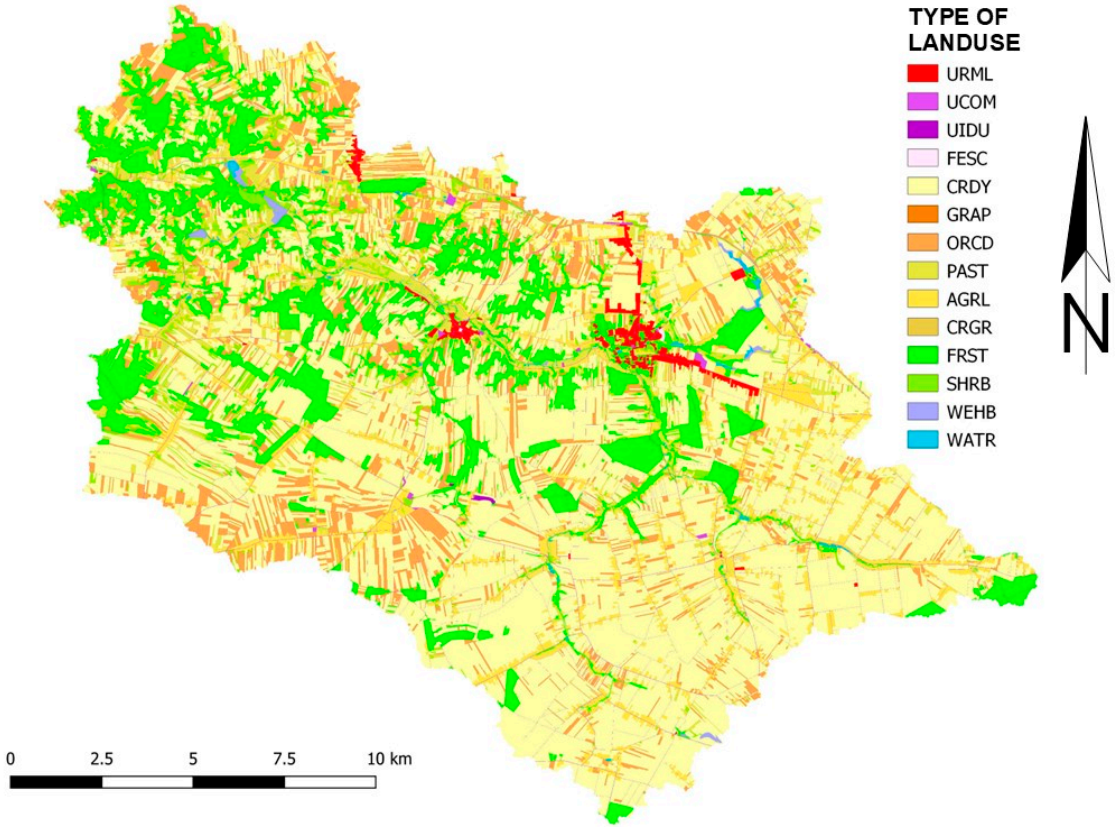

Figure 4. Land cover and use map of Bystra basin (own study).

The largest part of agricultural land is arable land beyond the range of irrigation facilities (52%), a large area is also orchards and plantations (11%), complex systems of cultivating plots (9%) and meadows and pastures (6%) (Table 2).

Table 2. Division of the cover and use as well as the percentage of use in the Bystra basin generated in the QSWAT interface (own study).

Corine Land Cover Legend	CLC	SWAT	[%]
	Code	Code	Part
Discontinuous urban fabric	112	URML	0.9
Industrial or commercial units	121	UCOM	1.6
Mineral extraction sites	131	UIDU	0.1
Sport and leisure facilities	142	FESC	0.1
		SUM=	**3**
Non-irrigated arable land	211	CRDY	52.4
Vineyards	221	GRAP	0.1
Fruit trees and berry plantations	222	ORCD	10.9
Pastures	231	PAST	5.9
Complex cultivation patterns	242	AGRL	9.0
Land principally occupied by agriculture, with signifi-cant areas of natural vegetation	243	CRGR	0.1
		SUM=	**78**
Mixed forest	313	FRST	16.3
Transitional woodland-shrub	324	SHRB	2.4
Inland marshes	411	WEHB	0.3
Water courses	511	WATR	0.3

3. Methods

3.1. SWAT and SWAT-CUP

In order to examine the water balance of the Bystra River catchment area, the soil and water assessment tool (SWAT) model was used [32]. The SWAT model can be used with a variety of computer programs. For the purpose of this article, the QSWAT3 v1.1 model with interface in Quantum GIS 3.10.13 Coruna [33] was used. SWAT Editor 23 October 2012 software [34] was used for model calculations. The SWAT model is a deterministic model developed for the US Department of Agriculture [35] that is based on mapping physical, chemical, and biological processes using mathematical formulas, developed to predict the effects of management practices on water and agricultural chemical yields on a basin scale [36,37].

The water balance is the basis and the driving force behind all of the processes that take place in the catchment area, regardless of the type of analysis performed with the use of the SWAT model [38]. The modeling of the watershed is carried out in two phases: a land phase and routing phase. The land phase of the hydrological cycle [39] controls the amount of water, sediment, nutrients and pesticides entering the main canal in each catchment area. The land phase of the hydrological cycle controls the amount of water, sediment, nutrients, and pesticides introduced into the main canal in each catchment area, covering long periods of time with a time resolution of one year, month, or day (Figure 5).

Routing phase of the hydrologic cycle which can be defined as the movement of water, sediments, etc. through the channel network of the watershed to the outlet. The hydrologic cycle can be defined as the movement of water, sediments, etc. through the channel network of the watershed to the outlet [40]. The simulated processes include the cycles of nitrogen, phosphorus, carbon, pesticides, bacteria, and metals. Above the processes are related in the SWAT model with the plant growth cycle and catchment management practices (e.g., plowing, fertilization, harvesting plants, irrigation of fields, collection and transfer

of water, drainage of water and sewage, use of home sewage treatment plants, and buffer zones along watercourses) [32,41].

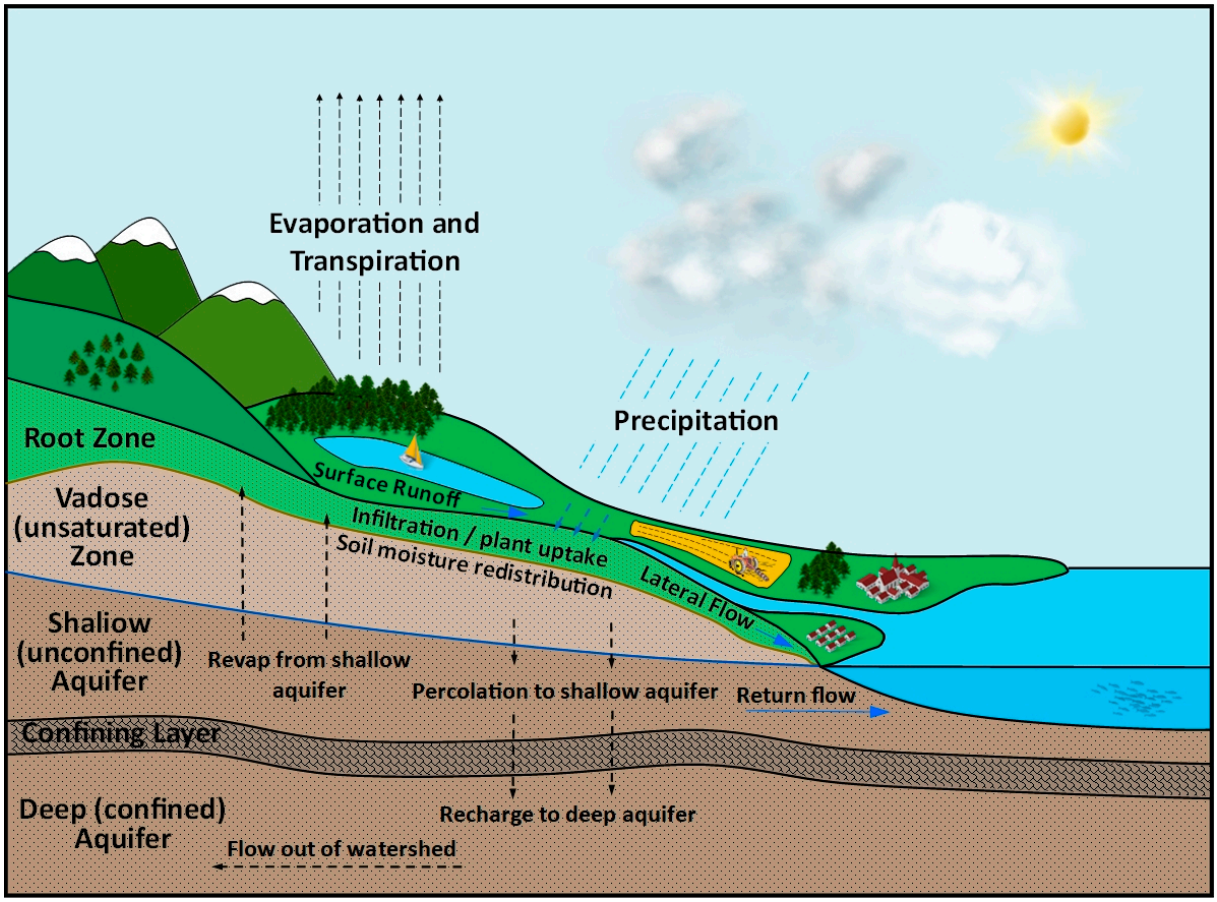

Figure 5. Schematic illustration of the conceptual water balance model in SWAT (own study).

The land phase estimates the runoff for each of these HRUs using the water balance equation:

$$SW_t = SW_0 + \sum_{i=1}^{t=T} (P_d - SURQ - E - w_{seep} - GWQ)$$

where SW_t is the final soil water content (mm); SW_0 is the initial soil water content (mm); t is time in days; P_d is precipitation (mm); $SURQ$ is surface runoff (mm); E is the evapotranspiration (mm); w_{seep} is amount of water entering the vadose zone from the soil profile (mm); and GWQ is groundwater flow (mm) [40].

The SWAT model used the Penman–Monteith method to assess potential evapotranspiration.

To better adjust (calibrate) the SWAT model to the actual conditions in the Bystra river catchment area, SWAT Calibration and Uncertainty Programs 5.2.1 [42] were used. The SWAT-CUP program is an instrument used to calibrate, analyze the uncertainty and sensitivity of the SWAT model [42,43]. The SUFI-2 algorithm was used since it works well for small catchments [44–46].

3.2. Data Used in the SWAT Model

To simulate the water balance in the SWAT model, spatial data were obtained from many sources, including:

- A digital elevation model covering the catchment area with a resolution of 5 m, obtained from the Central Geodetic and Cartographic Documentation Center [47];

- Data on the hydrography of the area (e.g., rivers, lakes, partial catchments), which were obtained from the Polish Hydrological Division Computer Map with descriptions [48];
- Data on sewage treatment plants [49];
- Digital soil and agricultural maps in digital form (scale 1:25,000 and 1:100,000) [50]; which were obtained from the Institute of Soil Science and Plant Cultivation in Puławy [51];
- Geological data describing lithology obtained from the Polish Geological Institute in the form of a Detailed Geological Map of Poland [27];
- Types of land cover and land use, digital data obtained from Corine Land Cover databases [52];
- A high-resolution orthophoto map published on the Geoportal in the form of WMS [53];
- Open Street Map data [54];
- Meteorological data obtained from IUNG in Puławy and the Institute of Meteorology and Water Management [55].

3.3. Adaptation of the SWAT Model for the Study Area

In the first stage, the input data for the precipitation-outflow system was prepared for SWAT modeling. Based on the digital elevation model and the location of the lakes in the studied area and water discharges from the wastewater treatment plant, a division of the Bystra River basin into partial catchments was generated in the SWAT editor. The editor generated 31 partial catchments (Figure 6). According to MPHP, the catchment area of the Bystra River consists of 21 sub-basins. The increased number of partial catchments is related to selecting points representing reservoirs and points source, for which additional data will be entered at a later stage. The above points must be located as close as possible to the line representing the river network. There are also many water reservoirs, ponds, and ponds in the sub-catchments that are not related to the watercourse line. These are the objects for which additional data will also be entered, representing all water reservoirs in the sub-catchment.

In the next stage of creating the SWAT model, hydrologic response unit (HRU) areas had to be generated, HRUs are homogeneous hydrological areas created on the basis of overlapping land cover maps, soil maps and slope maps [40].

For the needs of the SWAT model, a soil map of the Bystra catchment was developed based on digital soil and agricultural maps (scale 1:25,000 and 1:100,000) and geological data describing lithology. Data describing the parameters of the soils in the Bystra river catchment area were obtained as part of the statutory projects of IUNG-PIB [21].

During the preparation of soil data, it was also taken into account that the available water capacity and wilting point values were appropriate for the soils of the Bystra catchment area. These values were obtained from the study "Assessment of Water Retention in Soil and the Risk of Drought Based on the Water Balance for the Area of the Lower Silesia Voivodship", developed in 2013 by the employees of the Department of Soil Science, Erosion, and Land Protection IUNG-PIB in Puławy [20].

Due to the low detail of the Corine Land Cover map, additional vectorization of the cover and land use of the Bystra River catchment area was performed in order to increase the resolution of land use using an orthophoto map and Open Street Map data.

For the Bystra River catchment area, a division was also made due to the decline in the area in the following ranges: 0–6%, 6–10%, 10–18%, 18–27%, >27%. Slope ranges originate from the PWER and AWER indicators [56] for soil erosion risk, remaining as standard in terrain relief visualization in Poland. The Bystra River catchment area is similar to that of the Grodarz catchment area to the south, which has the same slope distribution. [57,58]. The Bystra River basin is similar in relief to the Grodarz River basin. In the studied catchment area, flat and slightly undulating areas with slopes up to 6% (72% of the catchment area) prevail. Steep slopes, from 6% to 10%, account for 11% of the catchment area. A small area of the catchment area is represented by land with falls from 10% to 27% (11%). A total of 6% of the catchment area are falls over 27%.

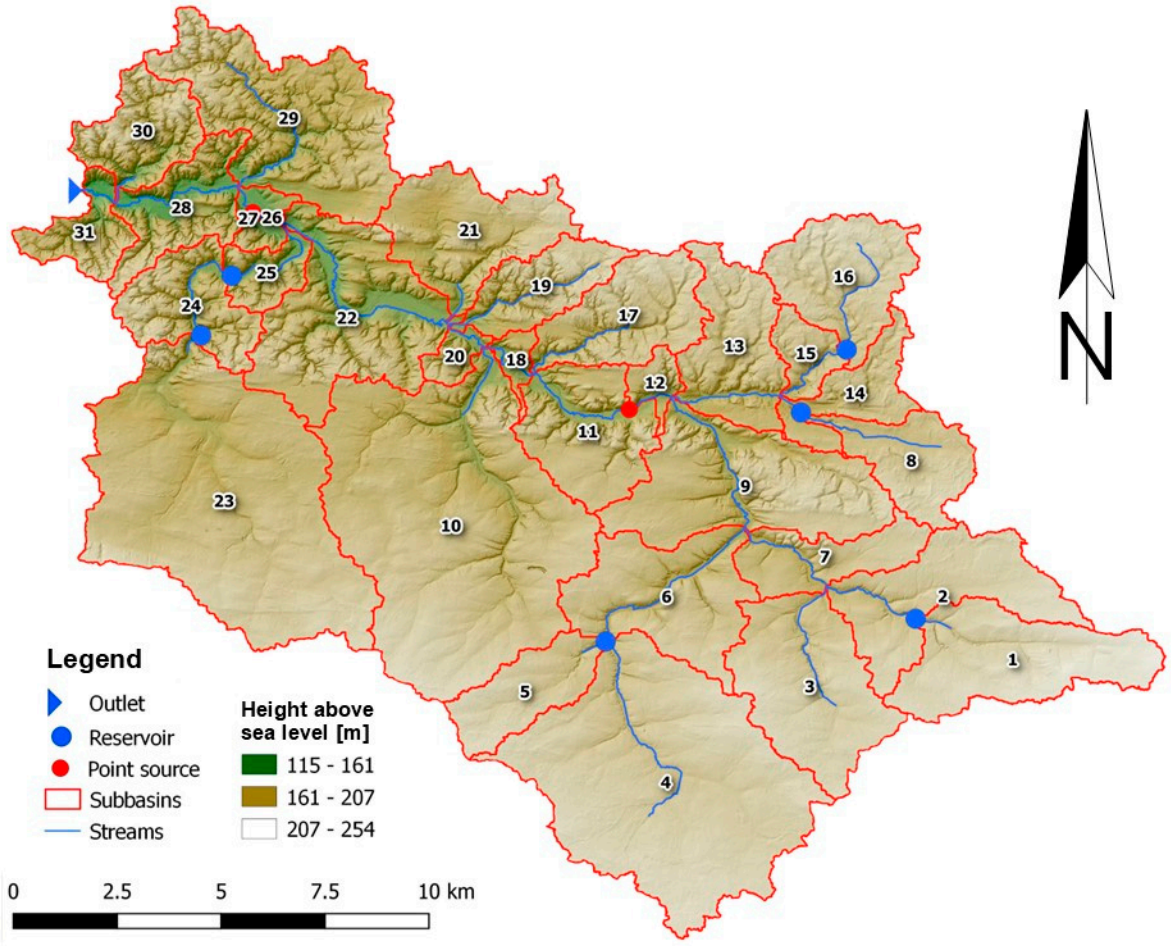

Figure 6. Study area: Bystra River basin with marked main tributaries and their catchments (own study).

After preparing the rasters for soil, land cover, and slopes, the catchment area was divided into HRU areas in the SWAT program.

During the creation of HRU in the SWAT program, the percentage of arable land outside the range of CRDY irrigation devices was separated from winter crops WWHT (43%), spring BARL crops (31%), canola CANP (14%) and other CRDY (12%), based on the publication Agriculture in the Lubelskie Voivodeship in 2019 [59]. From fruit orchards, ORCD was separated on the basis of the above-mentioned APPL apple orchards publication. Forests, on the other hand, were divided into coniferous FRSE forests (49%), deciduous FRSD forests (13%) and mixed FRST forests (38%) according to information obtained from the Regional Directorate of State Forests in Lublin [60].

A total of 484 HRU areas were generated. The HRU areas will be used at a later stage to build the SWAT model.

3.4. Meteorological Data

In the next stage of creating the SWAT model, the following meteorological data had to be loaded: sums of daily precipitation [mm]; daily minimum and maximum air temperature [°C]; average daily wind speed [m/s]; daily mean relative humidity; daily sums of total solar radiation [MJ/m^2]. Meteorological data were obtained from Pulawy weather station (Table 3). The data were prepared in SWAT Weather Database 0.18.03 [61].

Table 3. Meteorological data for the Bystra river basin (own study).

Weather Station	Measurement Period				
	Rainfall [mm]	**Temperature [°C]**	**Wind Speed [m/s]**	**Humidity**	**Solar Total Radiation [MJ/m^2]**
Pulawy	2005–2017	2005–2017	2005–2017	2005–2017	2005–2017
Rogalow	2005–2017	–	–	–	–
Lublin Radawiec	2005–2017	2005–2017	2005–2017	2005–2017	–

In the last stage of the SWAT model construction, some parameters related to point sewage discharges concerning water reservoirs outside the river network, concerning reservoirs, and parameters scheduled management operations for non-irrigated arable land were supplemented and corrected.

The parameters of rivers in the sub catchments were also improved on the basis of data obtained as part of the statutory projects of IUNG-PIB, as the automatically generated parameters of rivers regarding the length, depth, and width of the rivers were overestimated.

The current value of CO_2 concentration was also inserted in the prepared SWAT model.

After entering all of the necessary data into the SWAT model, a simulation of the water cycle in the Bystra River catchment was performed for 2010–2017 with a five-year model start-up period, in a monthly step.

3.5. SWAT CUP Calibration and Validation Results

After the SWAT simulation, the obtained model had to be calibrated in the SWAT-CUP program [62–64] to obtain a more accurate representation of the model with reality. For this purpose, data on average monthly flow velocities [m^3/s] in the vicinity of the estuary of the Bystra River basin to the Vistula for the years 2010–2014 were used, obtained under the statutory projects of IUNG-PIB. After receiving a satisfactory calibration, the model was validated using the data on the monthly average flow velocities [m^3/s] near the mouth of the Bystra River basin to the Vistula for 2015–2017, obtained under the statutory projects of IUNG-PIB. Calibration and validation were performed in a monthly step.

As a result of the calibration in the SWAT-CUP software, the best-fit parameter ranges were obtained that meet the accuracy requirements of calibration and validation [43,65,66].

The figure shows only the months which the water discharge was recorded and compared to the values simulated in 95 Percent Prediction Uncertainty (Figure 7). For the performed calibration and validation, there are data gaps in the measurements covering the periods from December 2010 to March 2013, September 2013 to January 2014, March 2015, July and August 2016, and from October 2016 to February 2017 and September 2017.

In addition to the above-mentioned best fit parameters, there are other parameter sets that can also give a good calibration result [63].

The Nash-Sutclif model efficiency coefficient (NSE) for calibration is in the range of $0.5 < \text{NSE} \leq 0.65$ and is a satisfactory result. The coefficient of determination R^2 is also within the acceptable range of $0.5 < \text{NSE} \leq 0.65$ [65]. The Nash-Sutclif model efficiency coefficient for the validation is in the range of $0.65 < \text{NSE} \leq 0.75$, which is good result. The coefficient of determination R^2 is in the range of $0.5 < \text{NSE} \leq 0.65$. This is also a satisfactory result [65].

For the performed calibration and validation, there are data gaps in the measurements covering the periods from December 2010 to March 2013, September 2013 to January 2014, March 2015, July and August 2016, from October 2016 to February 2017 and September 2017.

An important aspect is the appropriate consideration of the flow measurement period for validation and calibration. When preparing the data, the measurement data should be selected so that they cover a homogeneous period of time in terms of constant weather conditions. When preparing the data for the SWAT model, a distinction is made between

the so-called dry and wet years. If there are measurement series covering dry and wet years, then calibration and validation may be difficult [67].

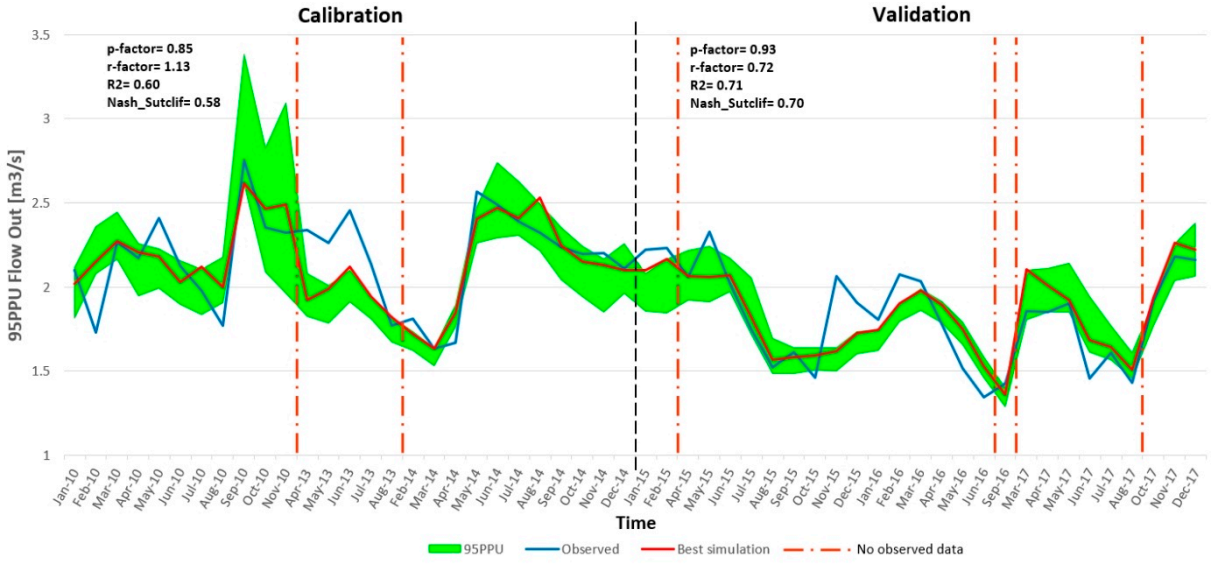

Figure 7. 95ppu plot and observed streamflow during calibration and validation (own study).

During the analysis of the results, the obtained values of potential evapotranspiration were also compared with the results of statutory IUNG-PIB research conducted as part of the Agricultural Drought Monitoring System project [68]. The SWAT model is a good representation of potential evapotranspiration in the studied area. In addition, the results of soil water content were compared with the available water capacity and wilting point values obtained from the study "Assessment of Water Retention in Soil and Drought Risk Based on the Water Balance for the Lower Silesian Voivodeship", developed in 2013 by employees of the Department of Soil Science, Erosion and Land Protection. IUNG-PIB in Pulawy [20].

3.6. Climate Change Scenarios

The daily gridded climate data for the period (2020–2050) with a spatial resolution of 0.11° were obtained from the EURO-CORDEX database that are openly available through the ESGF (Earth System Grid Federation, https://esgf-data.dkrz.de/search/cordex-dkrz, accessed on 10 February 2022) for Europe [69,70]. Climate projections (of daily minimum and maximum air temperature, precipitation, surface downwelling shortwave radiation, wind speed, relative humidity) that were used in SWAT model were extracted from grid cells that corresponds to the weather station's location. The projections are based on three regional climate models (RCMs) and two Representative Concentration Pathways (RCP). The RCMs (Regional Climate Models) were: RACMO22E, HIRHAM5 and RCA4 driven by one GCM (General Circulation Model): EC-EARTH. The RCPs correspond to a radiative forcing value in the year 2100 relative to pre-industrial values of +4.5 W m^{-2} (RCP4.5), while RCP8.5 to + 8.5 W m^{-2} (RCP8.5) [71,72] (Table 4).

In total we used six climate projections (three RCMs × two RCPs). The air temperature and precipitation data were additionally bias adjusted by the SMHI (Swedish Meteorological and Hydrological Institute) using DBS (distribution-based scaling) method [73] and regional reanalysis MESAN (mesoscale analysis) dataset from period 1989–2010 [74]. Since the downloaded data were performed on the rotated polar grid, we applied bilinear interpolation to remap this dataset to regular geographic latitude/longitude grid by using CDO (climate data operators) software [75].

Table 4. Description of the climate scenarios (own study).

Models	Scenario Assumptions		Brief Description of Climate Projections for Radiative Forcing	
GCM/RCM simulation	Increase in the maximum daily temperature	Increase in rainfall	RCP4.5	RCP8.5
			+4.5 W m^{-2}	+8.5 W m^{-2}
EC-EARTH/RACMO22E	+1.3 °C	+9%	RCP 4.5.1	RCP 8.5.1
EC-EARTH/HIRHAM5	+0.6 °C	+3%	RCP 4.5.2	RCP 8.5.2
EC-EARTH/RCA4	+0.9 °C	+5%	RCP 4.5.1	RCP 8.5.3

For the control period of the results of climate projections (RCP 4.5, RCP 8.5), validation was performed with existing observation data of temperature and precipitation (Table 5). The range of differences between the temperatures varies from 0.3 to 0.7 degrees Celsius in the plus. On the other hand, the differences for the climate projections in the control years 2010–2017 are smaller than 11% to 22% percent compared to the observational data.

Table 5. Validation of meteorological data (temperature and precipitation) (own study).

Temperature [°C]								Precipitation [mm]							
Climate model	Observation data	RCP 4.5.1	RCP 4.5.2	RCP 4.5.3	RCP 8.5.1	RCP 8.5.2	RCP 8.5.3	Climate model	Observation data	RCP 4.5.1	RCP 4.5.2	RCP 4.5.3	RCP 8.5.1	RCP 8.5.2	RCP 8.5.3
Time interval		2010–2017						Time interval		2010–2017					
Annual average	9.1	9.5	9.6	9.7	9.6	9.7	9.9	Annual sum	604	543	560	512	549	517	491
		+0.3	+0.5	+0.5	+0.5	+0.5	+0.7			−14%	−11%	−19%	−13%	−18%	−22%

The prepared model, after calibration and validation, was used for research related to the RCP 4.5 and RCP 8.5 climate change scenarios (changes in carbon dioxide concentration in the future decades) [70,76,77] which scenarios have been accepted by the International Panel on Climate Change [78].

For each of the projections, there is a certain confidence interval of the flow result obtained in the SWAT-CUP program. In order to compare the climate change scenarios for individual climate projections (RCP 4.5.1, RCP 8.5.1, RCP 4.5.2, RCP 8.5.2, RCP 4.5.3 and RCP 8.5.3), one iteration was carried out in SWAT-CUP for the best calibration parameters for 2020–2050 for prepared scenarios (Table 4). Additionally, for the RCP 4.5 and RCP 8.5 scenarios, changes in CO_2 concentrations in individual decades were adopted: 2021–2030, 2031–2040 and 2041–2050, developed by the Potsdam Institute for Climate Impact Research [79,80].

4. Average Annual Prospects of Climate Scenarios RCP 4.5 and RCP 8.5 for the Period 2020–2050

The average annual sum of precipitation and the average annual temperature in the years 2000–2050 are different for different projections in the RCP 4.5 and RCP 8.5 climate scenarios (Figure 8). For the projection RCP 4.5.1, RCP 8.5.1, and RCP 8.5.2 the trend of average annual precipitation will be slightly increasing in the following years. On the other hand, for the RCP 4.5.2 projection, the trend of average annual precipitation totals will be slightly decreasing. For the RCP 4.5.3 and RCP 8.5.3 projection, the trend of average annual precipitation totals will be increasing.

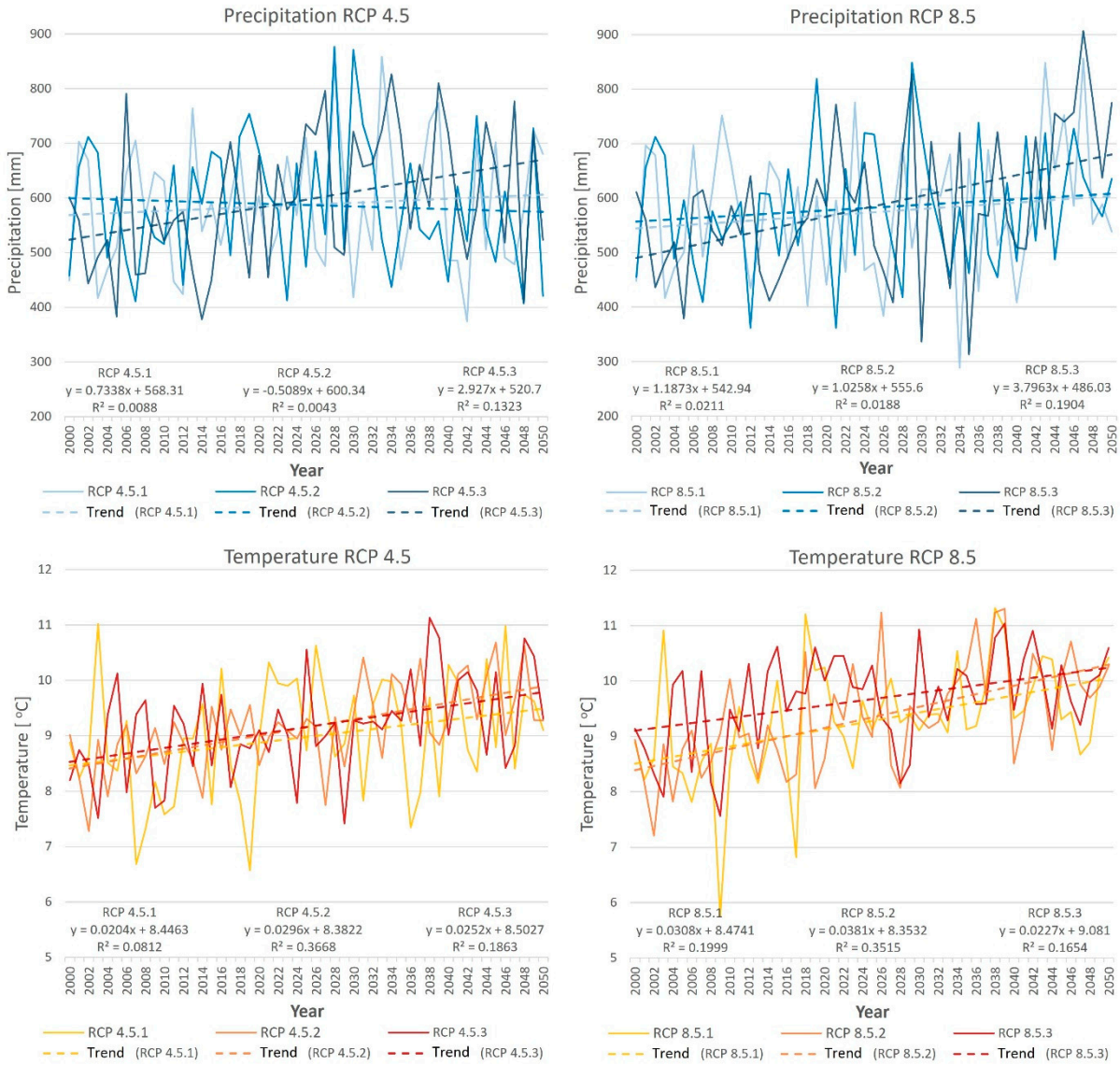

Figure 8. The average annual sum of precipitation and the average annual temperature in the Bystra River catchment area in the years 2000–2050 for individual climate projections in the RCP 4.5 and RCP 8.5 scenarios with trend lines (own study).

For the RCP 4.5 and RCP 8.5 scenarios, all three forecasts will see an increase in the annual mean temperature trend in the coming decades.

The trend of the average annual number of days without precipitation for the RCP 4.5 scenarios for all projections and for the RCP 8.5.2 projection are positive. However, in the case of RCP 8.5.1 and RCP 8.5.3 there is no trend line (Figure 9).

The trend of the average annual number of days with an average temperature above 5 °C in the years 2020–2050 for most climate projections is positive, apart from the RCP 4.5.1 projection.

The average monthly sums of precipitation for the Bystra River basin in the simulation years 2010–2017 and change in the individual climate change projections in the years 2021–2030, 2031–2040, and 2041–2050 are shown in Table 6. These changes are especially visible in March, August, and November, where for most of the projections there is an increase in the average monthly precipitation.

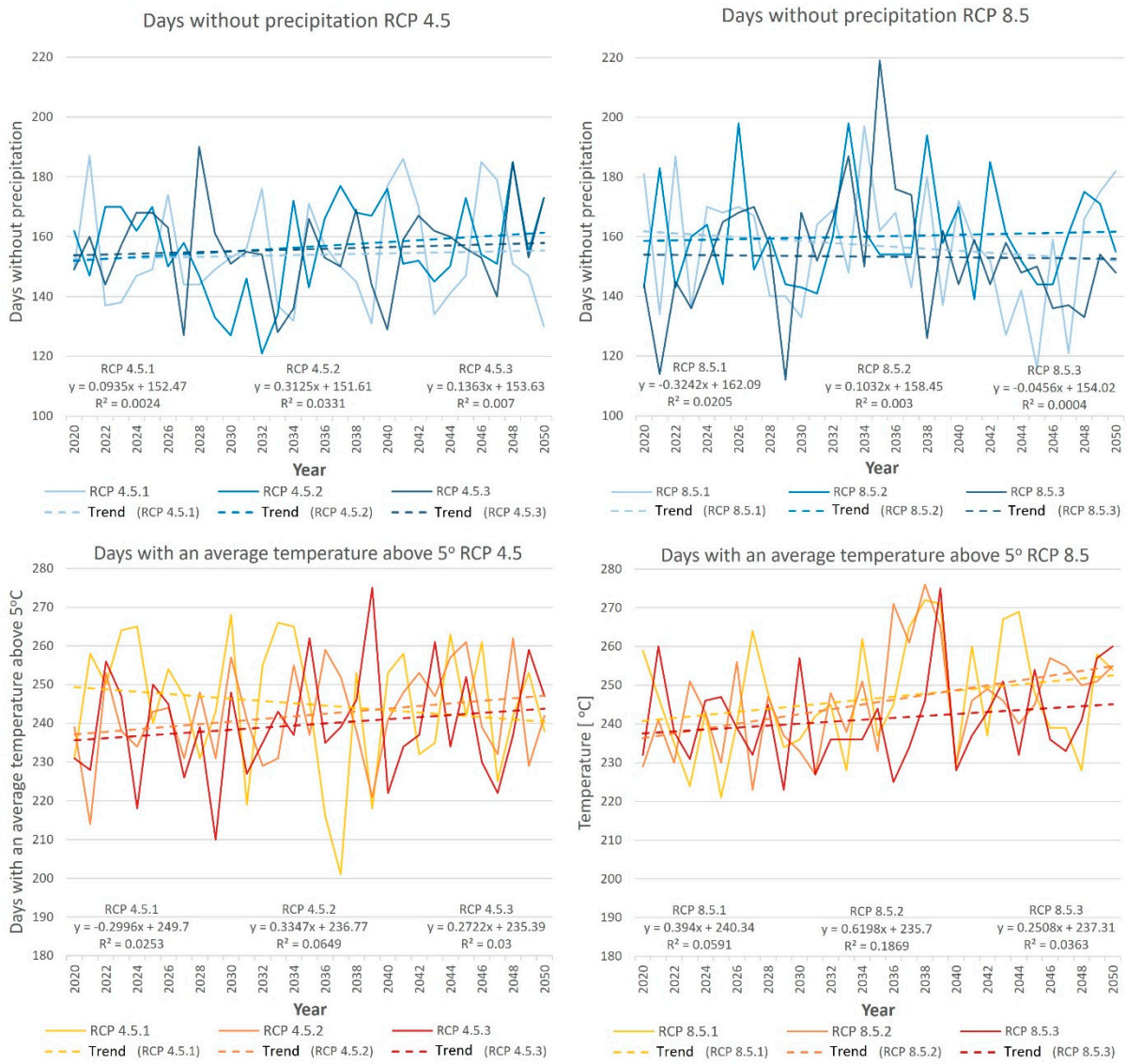

Figure 9. The average annual sum of days without precipitation and the average annual sum of days with temperatures above 5 °C in the Bystra River basin in the years 2020–2050 for individual climate projections in the RCP 4.5 and RCP 8.5 scenarios together (own study).

On the other hand, the decrease in average monthly sums of atmospheric precipitation will occur in most of the projections in January, May, July, and October.

For most of the projections, the average annual precipitation will be lower in the next decades as compared to 2010–2017. Larger annual mean sums will appear in the forecasts RCP5.1 (2031–2040), RCP 4.5.2 (2021–2030), RCP 4.5.3 (2021–2030, 2031–2040, 2041–2050), RCP 8.5.2 (2021–2030, 2041–2050), RCP 8.5.1, and RCP 8.5.3 (2041–2050).

Annual averages for RCP 2041–2050 for RCP 4.5 are lower by 3%, while for RCP 8.5 they are higher by 11% compared to the lower period.

Table 6. Comparison of the average distribution of precipitation in individual months for the SWAT simulation period 2010–2017 with individual projections for the RCP 4.5 and RCP 8.5 climate change scenarios for the periods 2021–2030, 2031–2040, and 2041–2050 (own study).

Climate Model	SWAT	RCP 4.5.1	RCP 4.5.2	RCP 4.5.3	RCP 8.5.1	RCP 8.5.2	RCP 8.5.3	RCP 4.5.1	RCP 4.5.2	RCP 4.5.3	RCP 8.5.1	RCP 8.5.2	RCP 8.5.3	RCP 4.5.1	RCP 4.5.2	RCP 4.5.3	RCP 8.5.1	RCP 8.5.2	RCP 8.5.3
Time Interval	**2010–2017**	**2021–2030**						**2031–2040**						**2041–2050**					
Month	**Average Monthly Precipitation [mm]**																		
January	33	25	30	28	24	27	32	31	44	33	21	29	38	24	33	22	23	41	39
		−25%	−10%	−15%	−25%	−16%	−3%	−5%	+36%	+2%	−36%	−12%	+15%	−27%	+1%	−32%	−31%	+25%	+18%
February	29	22	32	31	27	30	28	20	32	34	21	33	29	16	34	32	27	28	36
		−24%	+11%	+10%	−5%	+6%	−3%	−30%	+12%	+17%	−28%	+16%	+1%	−43%	+19%	+11%	−5%	0%	+26%
March	32	29	44	43	39	37	44	49	46	58	28	41	34	47	41	43	41	59	39
		−11%	+38%	+34%	+22%	+14%	+36%	+51%	+44%	+80%	−13%	+27%	+6%	+46%	+26%	+34%	+28%	+83%	+21%
April	41	46	48	36	32	37	50	30	41	37	46	26	45	36	47	40	47	40	52
		+11%	+15%	−13%	−22%	−10%	+22%	−26%	−1%	−10%	+12%	−38%	+9%	−13%	+13%	−3%	+13%	−3%	+26%
May	82	62	68	75	64	62	61	66	40	66	67	48	69	58	61	75	96	80	74
		−25%	−17%	−9%	−22%	−24%	−25%	−20%	−51%	−19%	−19%	−42%	−16%	−30%	−26%	-8%	+17%	−2%	−10%
June	58	66	81	56	61	72	53	72	53	59	66	74	49	62	52	43	66	69	50
		+14%	+41%	−3%	+6%	+25%	−9%	+25%	−8%	+3%	+14%	+29%	−15%	+8%	−10%	−25%	+14%	+20%	−13%
July	95	114	69	80	83	85	53	130	96	124	62	82	64	96	74	80	62	63	82
		+21%	−27%	−15%	−13%	−10%	−44%	+38%	+1%	+31%	−35%	−14%	−32%	+1%	−22%	−15%	−34%	−33%	−14%
August	55	69	66	87	75	62	59	50	73	73	66	52	76	58	58	59	102	63	75
		+26%	+21%	+58%	+36%	+13%	+7%	−10%	+32%	+33%	+19%	−6%	+37%	+6%	+5%	+7%	+85%	+14%	+35%
September	57	55	47	81	43	51	95	68	52	78	47	43	63	67	65	73	53	70	107
		−3%	−16%	+43%	−23%	−10%	+67%	+21%	−8%	+37%	−16%	−24%	+12%	+18%	+14%	+28%	−6%	+24%	+89%
October	45	38	38	27	46	37	31	41	31	40	46	29	23	41	32	37	44	33	33
		−15%	−14%	−40%	+2%	−17%	−29%	−8%	−31%	−10%	+3%	−34%	−48%	−9%	−28%	−16%	−2%	−25%	−26%
November	34	33	66	42	31	69	41	30	35	45	49	54	35	29	32	58	49	50	68
		−4%	+95%	+24%	−8%	+103%	+22%	−11%	+2%	+31%	+43%	+58%	+3%	−14%	−5%	+71%	+43%	+47%	+99%
December	36	29	30	41	30	33	41	41	23	43	29	35	41	39	32	37	38	26	57
		−20%	−16%	+13%	−18%	−8%	+14%	0%	−36%	+18%	−21%	−4%	+14%	0%	−11%	+2%	+4%	−29%	+59%
Annual sum	596	586	621	627	556	604	588	628	566	690	546	545	566	573	561	600	647	622	712
		−2%	+4%	+5%	−7%	+1%	−1%	+5%	−5%	+16%	−8%	−9%	−5%	−4%	−6%	+1%	+9%	+4%	+19%

By analyzing the spatial distribution of changes in the average annual precipitation total in 31 sub-catchments for the simulation period in 2010–2017 compared to the period 2041–2050 (Figure 10) in the RCP 4.5.1 and RCP 4.5.3 climate projections, the precipitation total will decrease by several percent in north-west and south-east region. In the RCP 4.5.2 projection, a reduced amount of precipitation will occur in the entire catchment area, while in the RCP 8.5.2 projection it will occur only in the northwestern part. In projections 8.5.1 and 8.5.3, an increased amount of precipitation, up to 23%, will be present in the entire area in the period 2041–2050. Most of the RCP 8.5.2 area will also have an increased amount of precipitation.

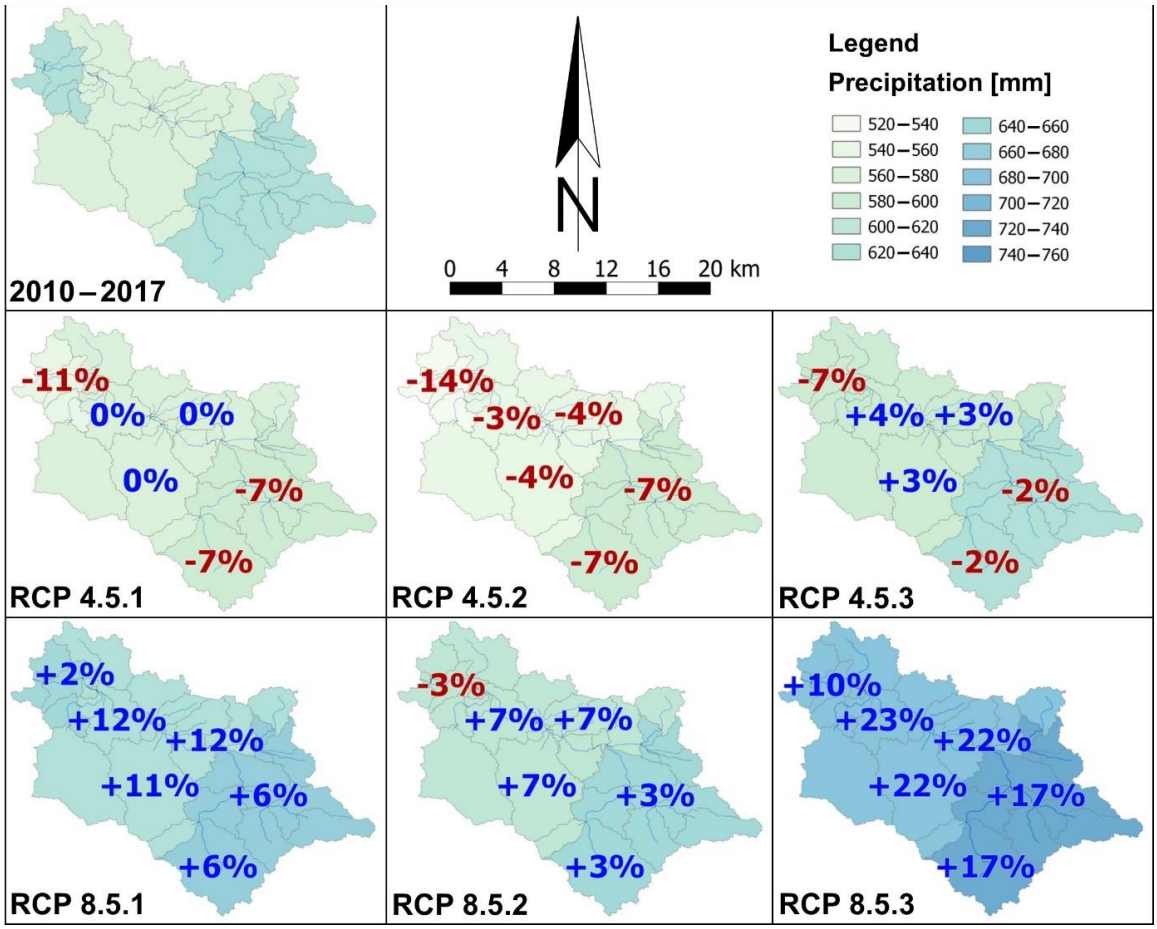

Figure 10. Comparison of the average annual sum of precipitation in 31 sub-catchments for the SWAT simulation period for 2010–2017 and 2041–2050 for individual climate projections in the RCP 4.5 and RCP 8.5 scenarios (own study).

The average monthly temperature distributions for the Bystra River basin in the 2010–2017 simulation years also change compared to the individual climate change projections in 2021–2050 (Table 7). These changes are especially visible in November and December, where for most of the projections the average monthly temperature is lower than in the 2010–2017 simulation period. On the other hand, in January, April, May, September, and October, the average monthly temperatures are higher for most of the projections. For the RCP 8.5.2 (2031–2040, 2041–2050) and RCP 8.5.3 (2041–2050) projections, the average monthly temperatures for most months are higher than in the 2010–2017 simulation years.

The temperature in the 2041–2050 decade for RCP 4.5 will be higher by an average of 0.4 °C, while for RCP 8.5 it will be higher by an average of 0.8 °C compared to the simulation period.

Table 7. Comparison of the average temperature distribution in individual months for the SWAT simulation period 2010–2017 with individual projections for the RCP 4.5 and RCP 8.5 climate change scenarios for the periods 2021–2030, 2031–2040, and 2041–2050 (own study).

Climate Model	SWAT	RCP 4.5.1	RCP 4.5.2	RCP 4.5.3	RCP 8.5.1	RCP 8.5.2	RCP 8.5.3	RCP 4.5.1	RCP 4.5.2	RCP 4.5.3	RCP 8.5.1	RCP 8.5.2	RCP 8.5.3	RCP 4.5.1	RCP 4.5.2	RCP 4.5.3	RCP 8.5.1	RCP 8.5.2	RCP 8.5.3
Time Interval	**2010–2017**	**2021–2030**						**2031–2040**						**2041–2050**					
Month	**Average Monthly Temperature [°C]**																		
January	−2.9	−0.2	0.9	−2.8	−2.9	−2.3	−2.0	−3.0	0.1	0.4	−0.8	−0.4	0.7	−0.9	0.0	−2.3	−2.3	0.6	0.1
		+2.7	+3.7	0.0	−0.1	+0.5	+0.9	−0.1	+2.9	+3.3	+2.0	+2.5	+3.5	+2.0	+2.9	+0.6	+0.6	+3.5	+3.0
February	−0.9	2.1	−2.0	−0.9	−0.3	0.8	0.1	0.3	0.0	0.5	1.8	1.0	3.0	−0.9	0.4	2.3	0.7	0.6	2.9
		+3.0	−1.1	0.0	+0.6	+1.7	+1.0	+1.2	+0.9	+1.4	+2.7	+1.9	+3.9	0.0	+1.3	+3.2	+1.6	+1.5	+3.8
March	4.2	6.3	1.8	5.2	4.3	4.1	3.5	3.6	3.4	4.0	5.9	4.5	4.8	3.8	3.5	4.7	5.0	3.8	5.0
		+2.2	−2.4	+1.1	+0.1	−0.1	−0.7	−0.5	−0.7	−0.1	+1.7	+0.3	+0.7	−0.4	−0.7	+0.6	+0.9	−0.3	+0.9
April	9.4	9.9	8.2	9.1	11.3	9.4	8.3	11.0	8.4	9.8	10.7	9.3	9.8	10.9	9.3	8.3	12.1	9.2	9.8
		+0.5	−1.3	−0.3	+1.9	−0.1	−1.1	+1.6	−1.1	+0.4	+1.3	−0.1	+0.4	+1.5	−0.1	−1.1	+2.7	−0.3	+0.3
May	14.5	15.1	13.8	14.6	16.2	15.0	14.7	14.0	15.1	15.2	16.0	15.7	16.1	16.1	15.6	15.0	14.5	15.0	16.0
		+0.5	−0.8	+0.1	+1.6	+0.4	+0.2	−0.6	+0.5	+0.7	+1.5	+1.2	+1.6	+1.5	+1.0	+0.5	0.0	+0.5	+1.5
June	18.0	17.2	16.8	17.7	16.9	18.0	17.0	17.6	18.3	17.4	16.7	18.6	19.1	18.4	19.1	17.8	17.5	17.6	18.8
		−0.8	−1.2	−0.3	−1.2	−0.1	−1.0	−0.5	+0.3	−0.7	−1.3	+0.5	+1.1	+0.4	+1.0	−0.2	−0.6	−0.4	+0.7
July	20.2	19.8	19.9	20.8	20.0	20.1	20.1	20.2	20.5	20.4	20.6	20.9	20.5	20.1	19.7	21.3	20.4	20.5	20.7
		−0.4	−0.3	+0.6	−0.1	−0.1	−0.1	0.0	+0.3	+0.2	+0.5	+0.7	+0.3	−0.1	−0.4	+1.1	+0.2	+0.4	+0.5
August	19.8	19.2	19.7	19.0	18.4	19.7	20.0	19.7	19.5	19.1	19.4	20.2	20.9	19.1	19.7	19.8	18.9	20.3	19.6
		−0.6	−0.1	−0.8	−1.4	−0.1	+0.2	0.0	−0.3	−0.7	−0.3	+0.4	+1.2	−0.7	−0.1	+0.1	−0.8	+0.5	−0.2
September	14.6	14.0	14.5	13.4	15.1	15.0	14.3	14.8	15.1	14.0	16.0	15.8	16.3	14.7	15.8	15.0	15.1	15.5	14.9
		−0.6	−0.1	−1.2	+0.5	+0.4	−0.3	+0.2	+0.5	−0.6	+1.4	+1.2	+1.7	+0.1	+1.2	+0.4	+0.5	+0.9	+0.3
October	8.6	9.1	10.1	8.7	8.4	9.6	9.6	8.5	10.4	9.4	9.7	9.8	10.7	9.0	10.0	9.8	10.6	11.3	10.4
		+0.5	+1.5	+0.1	−0.2	+1.1	+1.0	0.0	+1.8	+0.8	+1.2	+1.2	+2.2	+0.4	+1.4	+1.2	+2.0	+2.8	+1.9
November	4.9	3.2	4.5	3.8	4.9	3.8	4.5	3.9	3.8	3.8	3.8	4.0	4.3	3.7	3.4	4.3	3.3	4.1	5.0
		−1.6	−0.4	−1.0	0.0	−1.1	−0.4	−0.9	−1.1	−1.1	−1.1	−0.8	−0.6	−1.2	−1.5	−0.5	−1.5	−0.8	+0.1
December	0.4	0.0	−0.6	−1.6	−0.9	0.1	−0.8	−3.0	−0.1	1.4	−1.9	0.8	0.4	−1.2	1.4	−0.3	0.7	0.3	0.9
		−0.4	−1.0	−1.9	−1.2	−0.2	−1.2	−3.4	−0.5	+1.0	−2.2	+0.5	+0.1	−1.6	+1.0	−0.6	+0.3	−0.1	+0.5
Annual avearge	9.2	9.6	8.9	8.9	9.3	9.4	9.1	9.0	9.5	9.6	9.8	10.0	10.6	9.4	9.8	9.7	9.7	9.9	10.3
		+0.4	−0.3	−0.3	0.0	+0.2	−0.1	−0.2	+0.3	+0.4	+0.6	+0.8	+1.3	+0.2	+0.6	+0.4	+0.5	+0.7	+1.1

5. Results

The trend of the average annual sum of actual evapotranspiration in the years 2021–2050 in most of the projections (except for RCP 8.5.3) decreases slightly in the coming decades (Figure 11).

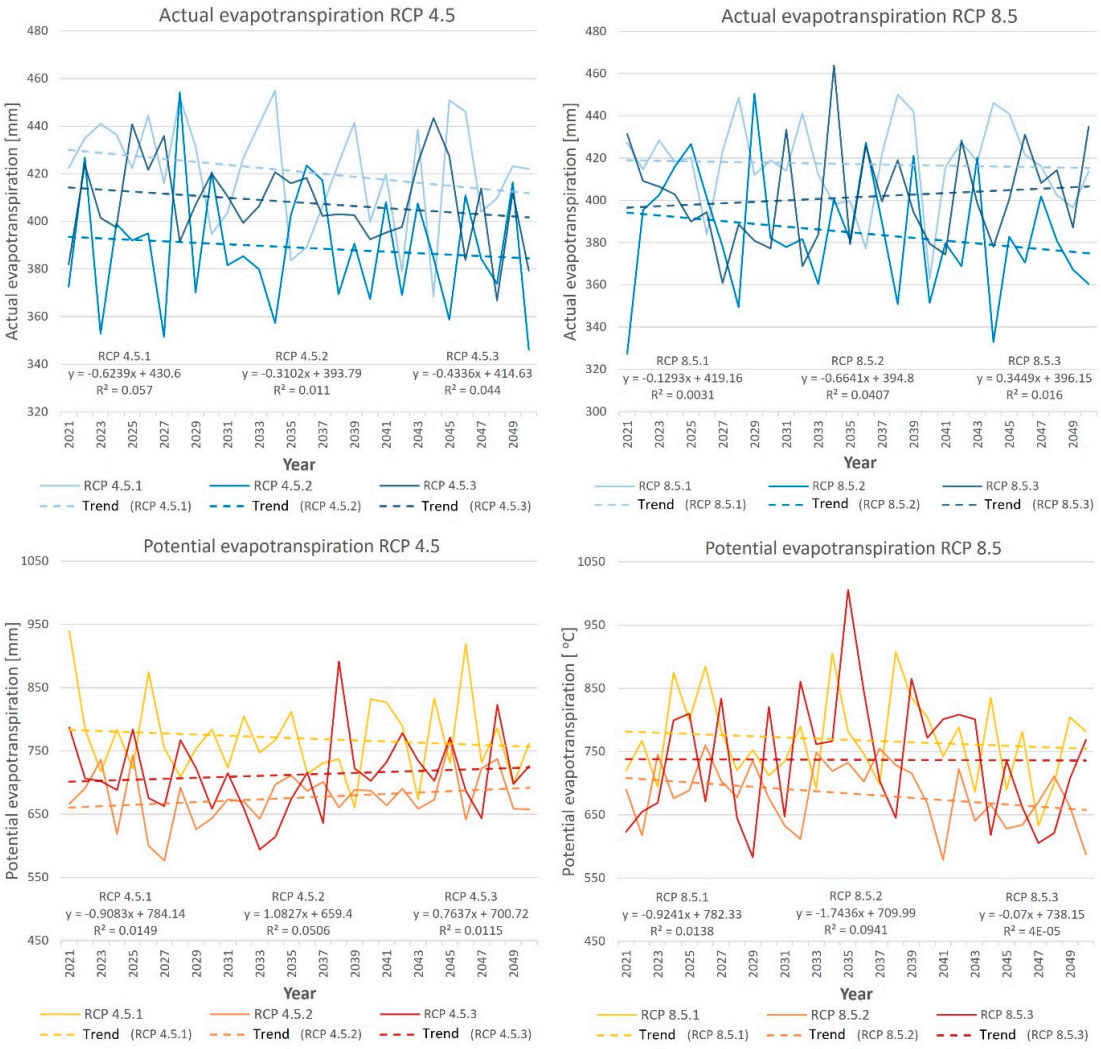

Figure 11. Average annual actual evapotranspiration and potential evapotranspiration in the catchment area of the Bystra River in the years 2021–2050 for individual climate projections in the RCP 4.5 and RCP 8.5 scenarios together with trend lines (own study).

The trend of the average annual sum of potential evapotranspiration in RCP 4.5.1, RCP 8.5.1 and RCP 8.5.2 projections will decrease in the coming decades. However, for the RCP 4.5.2 and RCP 4.5.3 projections, the trend is growing. The trend line for the RCP 8.5.3 projection does not change significantly.

The average monthly sum of actual evapotranspiration increases for all projections for most months compared to the simulation period 2010–2017. In June, for most projections, the average monthly sum of evapotranspiration will be lower than the average for 2010–2017 (Table 8).

The average annual potential evapotranspiration in the 2041–2050 decade for RCP 4.5 will be higher by an average of 8%, while for RCP 8.5 it will be higher by an average of 8% compared to the simulation period.

For potential evapotranspiration, the average monthly sum increases for most of the projections in all months compared to the 2010–2017 simulation period (Table 9).

Table 8. Comparison of the average monthly sum of actual evapotranspiration for the SWAT simulation period 2010–2017 with individual projections for the RCP 4.5 and RCP 8.5 climate change scenarios for the periods 2021–2030, 2031–2040, and 2041–2050 (own study).

Climate Model	SWAT	RCP 4.5.1	RCP 4.5.2	RCP 4.5.3	RCP 8.5.1	RCP 8.5.2	RCP 8.5.3	RCP 4.5.1	RCP 4.5.2	RCP 4.5.3	RCP 8.5.1	RCP 8.5.2	RCP 8.5.3	RCP 4.5.1	RCP 4.5.2	RCP 4.5.3	RCP 8.5.1	RCP 8.5.2	RCP 8.5.3
Time Interval	**2010–2017**	**2021–2030**						**2031–2040**						**2041–2050**					
Month	**Average Monthly Actual Evapotranspiration [mm]**																		
January	4	10	8	10	6	6	9	6	7	10	9	7	10	7	6	9	7	6	10
		+136%	+94%	+143%	+50%	+59%	+114%	+53%	+67%	+152%	+128%	+77%	+142%	+82%	+58%	+116%	+84%	+60%	+156%
February	9	17	11	14	14	12	15	15	9	15	17	12	16	13	12	15	15	10	16
		+91%	+19%	+60%	+55%	+30%	+68%	+69%	+0%	+67%	+88%	+35%	+77%	+45%	+31%	+72%	+70%	+11%	+78%
March	26	36	21	32	32	25	28	30	24	30	34	26	30	31	24	30	33	24	29
		+39%	−19%	+22%	+21%	−4%	+9%	+17%	−9%	+17%	+31%	0%	+16%	+18%	-+6%	+15%	+27%	−9%	+10%
April	44	49	42	40	51	46	44	53	46	42	51	44	46	51	51	41	53	40	43
		+11%	−4%	−9%	+16%	+5%	-1%	+20%	+4%	−4%	+17%	-1%	+4%	+16%	+15%	−7%	+21%	−10%	−2%
May	68	72	73	65	75	71	68	68	70	66	70	68	69	72	74	65	70	72	69
		+6%	+7%	−4%	+10%	+4%	0%	0%	+2%	−3%	+3%	-1%	+2%	+6%	+8%	−4%	+2%	+6%	+1%
June	62	54	64	58	56	60	57	54	58	55	51	58	53	55	56	56	55	59	50
		−12%	+4%	−6%	−10%	−3%	−8%	−12%	−6%	−12%	−18%	−6%	−14%	−11%	−10%	−10%	−12%	−5%	−20%
July	56	59	54	61	62	53	51	61	51	60	56	56	56	58	54	59	56	51	55
		+5%	−4%	+9%	+10%	−6%	−9%	+9%	−8%	+7%	-1%	0%	0%	+4%	−4%	+6%	0%	−9%	−2%
August	49	56	45	57	53	49	48	53	50	53	52	44	52	52	42	53	54	43	54
		+15%	−8%	+16%	+8%	0%	−2%	+7%	+3%	+8%	+6%	−11%	+5%	+7%	−14%	+8%	+10%	−13%	+9%
September	27	34	33	36	33	31	35	39	34	36	35	29	33	36	32	36	36	30	39
		+26%	+22%	+33%	+22%	+15%	+29%	+44%	+26%	+34%	+31%	+6%	+24%	+35%	+19%	+34%	+35%	+13%	+46%
October	16	23	24	20	21	18	21	21	20	19	21	19	22	22	19	22	22	22	21
		+44%	+51%	+31%	+33%	+15%	+35%	+33%	+29%	+24%	+32%	+22%	+38%	+42%	+24%	+42%	+43%	+39%	+35%
November	7	12	13	12	11	13	12	11	12	12	11	14	9	11	10	11	11	13	12
		+65%	+79%	+74%	+58%	+84%	+68%	+60%	+73%	+64%	+58%	+100%	+33%	+60%	+37%	+57%	+62%	+91%	+73%
December	4	8	7	7	7	9	7	6	7	9	4	9	9	7	6	7	6	7	8
		+98%	+72%	+54%	+62%	+107%	+60%	+0%	+66%	+119%	+5%	+101%	+104%	+0%	+48%	+66%	+51%	+60%	+94%
Annual sum	372	430	393	412	420	393	394	417	388	407	412	384	405	416	386	404	420	377	406
		+16%	+6%	+11%	+13%	+6%	+6%	+12%	+4%	+9%	+11%	+3%	+9%	+12%	+4%	+9%	+13%	+1%	+9%

Table 9. Comparison of the average monthly sum of potential evapotranspiration for the SWAT simulation period 2010–2017 with individual projections for the RCP 4.5 and RCP 8.5 climate change scenarios for the periods 2021–2030, 2031–2040, and 2041–2050 (own study).

Climate Model	SWAT	RCP 4.5.1	RCP 4.5.2	RCP 4.5.3	RCP 8.5.1	RCP 8.5.2	RCP 8.5.3	RCP 4.5.1	RCP 4.5.2	RCP 4.5.3	RCP 8.5.1	RCP 8.5.2	RCP 8.5.3	RCP 4.5.1	RCP 4.5.2	RCP 4.5.3	RCP 8.5.1	RCP 8.5.2	RCP 8.5.3
Time Interval	**2010–2017**	**2021–2030**						**2031–2040**						**2041–2050**					
Month	**Average Monthly Potential Evapotranspiration [mm]**																		
January	4	11	9	11	7	7	10	7	8	11	11	8	11	9	7	10	9	7	11
		+154%	+107%	+146%	+65%	+70%	+121%	+60%	+79%	+160%	+152%	+87%	+147%	+99%	+67%	+124%	+98%	+65%	+161%
February	10	22	12	16	16	15	17	18	10	18	22	14	19	17	13	18	18	11	19
		+124%	+21%	+64%	+61%	+48%	+77%	+86%	0%	+77%	+121%	+44%	+91%	+73%	+36%	+85%	+82%	+15%	+92%
March	35	60	27	44	42	34	35	42	30	40	52	36	45	43	31	42	45	30	39
		+70%	−24%	+23%	+19%	−6%	−1%	+19%	−15%	+14%	+46%	+2%	+26%	+22%	−12%	+18%	+26%	−14%	+11%
April	64	81	64	65	90	75	61	92	72	68	86	74	67	87	77	64	91	63	64
		+27%	0%	+2%	+40%	+17%	−4%	+44%	+12%	+6%	+35%	+16%	+5%	+36%	+21%	+1%	+42%	−2%	0%
May	92	111	103	98	114	107	98	102	111	97	110	109	103	115	111	93	95	100	98
		+21%	+12%	+6%	+24%	+15%	+5%	+11%	+20%	+5%	+19%	+18%	+11%	+24%	+20%	+1%	+3%	+8%	+6%
June	112	117	105	110	111	122	106	112	120	110	104	118	125	120	122	114	106	112	116
		+5%	−6%	−1%	−1%	+9%	−6%	0%	+7%	−1%	−7%	+6%	+12%	+7%	+10%	+2%	−5%	0%	+4%
July	119	127	126	135	137	124	137	128	120	121	139	121	136	136	117	133	140	118	127
		+7%	+6%	+13%	+15%	+4%	+15%	+8%	+1%	+2%	+17%	+2%	+15%	+15%	−1%	+12%	+18%	−1%	+6%
August	103	117	94	117	114	100	128	120	94	110	120	102	132	118	96	123	110	96	113
		+14%	−8%	+14%	+11%	−3%	+25%	+16%	−9%	+6%	+16%	0%	+29%	+15%	−7%	+20%	+7%	−7%	+10%
September	51	72	60	61	81	60	63	74	61	64	85	61	84	75	61	76	74	56	70
		+40%	+17%	+20%	+57%	+18%	+23%	+45%	+18%	+24%	+66%	+19%	+63%	+45%	+19%	+47%	+43%	+9%	+37%
October	23	39	36	35	36	30	34	35	34	30	40	32	44	35	32	37	36	34	33
		+70%	+56%	+56%	+60%	+30%	+48%	+54%	+49%	+31%	+74%	+39%	+95%	+53%	+39%	+61%	+60%	+48%	+44%
November	8	14	15	16	15	15	14	15	15	13	15	16	12	14	11	13	13	16	14
		+69%	+77%	+89%	+77%	+77%	+76%	+85%	+81%	+61%	+81%	+95%	+43%	+65%	+37%	+53%	+62%	+92%	+65%
December	5	10	8	7	8	10	7	6	8	10	5	10	9	7	7	8	7	8	9
		+113%	+79%	+55%	+75%	+117%	+62%	0%	+79%	+128%	+12%	+112%	+107%	0%	+60%	+68%	+54%	+69%	+92%
Annual sum	627	782	659	715	771	697	711	753	682	693	789	702	787	775	687	730	744	650	713
		+25%	+5%	+14%	+23%	+11%	+13%	+20%	+9%	+11%	+26%	+12%	+26%	+24%	+10%	+16%	+19%	+4%	+14%

The average annual potential evapotranspiration in the 2041–2050 decade for RCP 4.5 will be higher by an average of 12%, while for RCP 8.5 it will be higher by an average of 17% compared to the simulation period.

By analyzing the spatial distribution of changes in the average annual sum of actual evapotranspiration in 31 sub-catchments for the simulation period in 2010–2017 compared to the period 2041–2050 (Figure 12) for most projections, actual evapotranspiration will increase. Only for the projection of RCP 8.5.2 in the central part of the Bystra catchment area, the sum of actual evapotranspiration will be lower than in the simulation period.

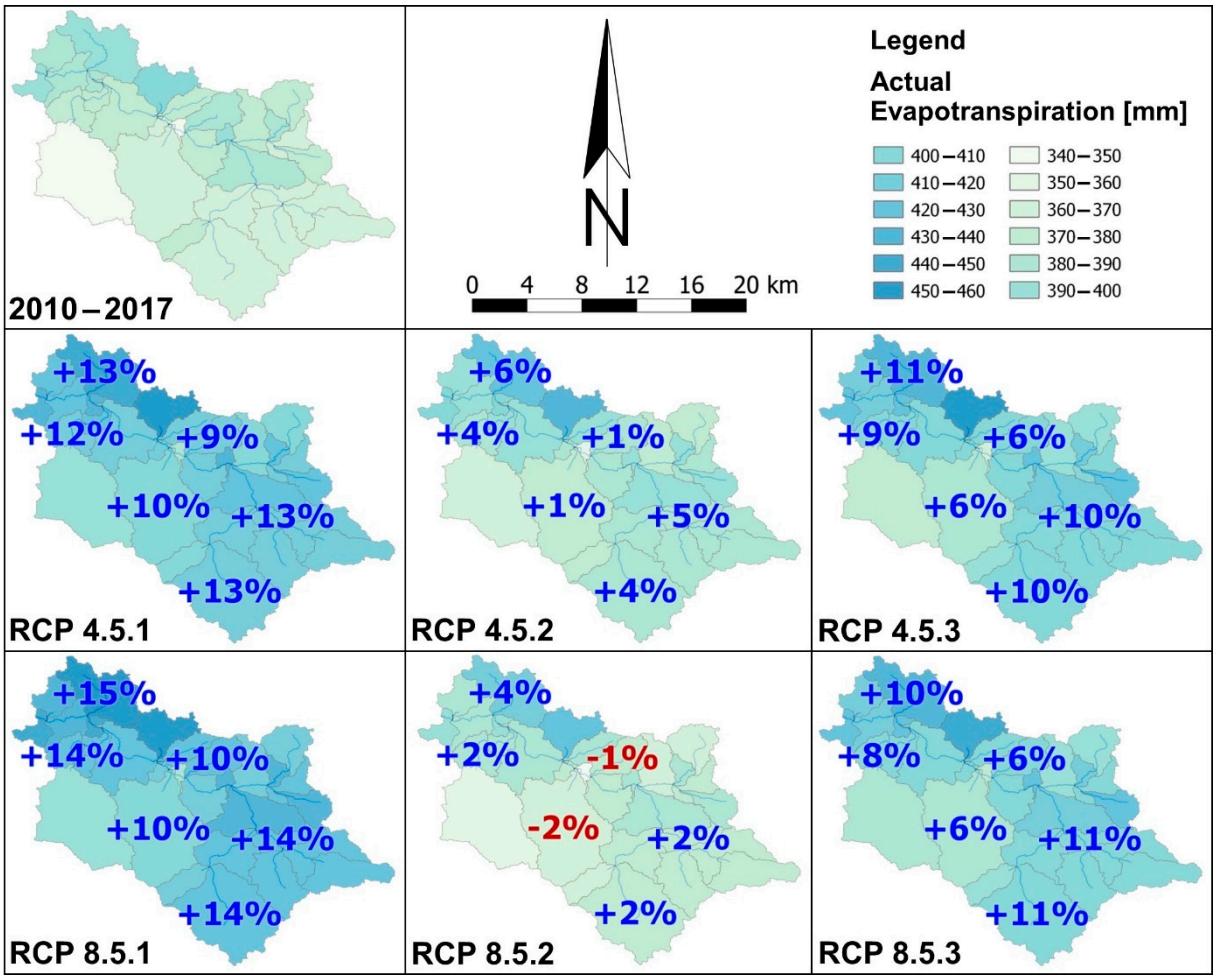

Figure 12. Comparison of the average sum of actual evapotranspiration in 31 sub-catchments for the SWAT simulation period for 2010–2017 and 2041–2050 for individual climate projections in the RCP 4.5 and RCP 8.5 scenarios (own study).

Spatial distribution of changes in the average annual sum of potential evapotranspiration in 31 sub-catchments for the simulation period in 2010–2017 compared to the period 2041–2050 (Figure 13) for all projections, the potential evapotranspiration will increase. The largest increase will be recorded in the RCP 4.5.1 and RCP 8.5.1 projections, reaching even 27% in the north-western part of the catchment area.

The trend of the average annual total runoff consisting of surface runoff, lateral flow and baseline flow in the RCP 8.5.1, RCP 8.5.2, and RCP 8.5.3 projections will increase over the years 2021–2050 (Figure 14). For the RCP 4.5.2 projection, the trend will be downward. However, for the RCP 4.5.1 and RCP 4.5.2 projections, the trend will not change significantly.

The average monthly total runoff for the Bystra River basin will be lower in most climate change projections in the years 2021–2030, 2031–2040, and 2041–2050 (Table 10). The exceptions will be the RCP 4.5.3 (2031–2040) and RCP 8.5.2, RCP 8.5.3 (2041–2050)

projections, where the average total monthly runoff will be higher compared to the 2010–2017 simulation years.

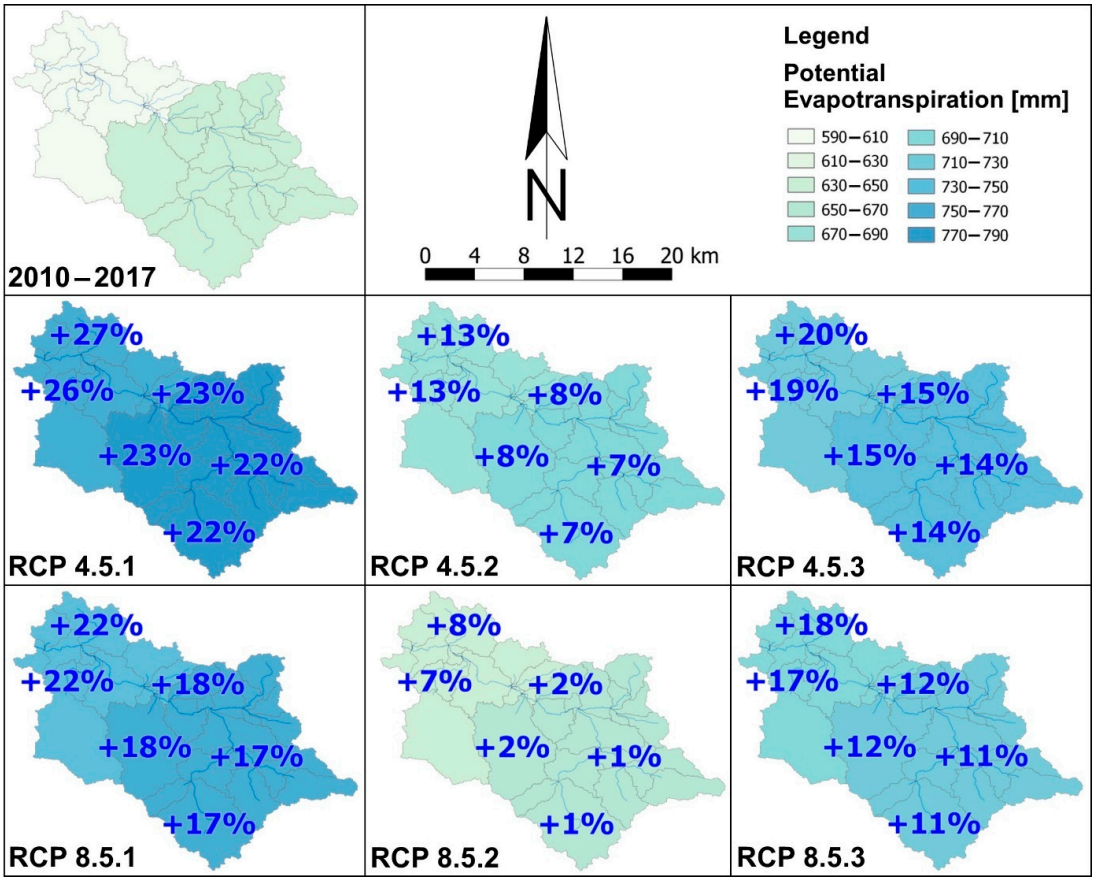

Figure 13. Comparison of the average sum of potential evapotranspiration in 31 sub-catchments for the SWAT simulation period for 2010–2017 and 2041–2050 for individual climate projections in the RCP 4.5 and RCP 8.5 scenarios (own study).

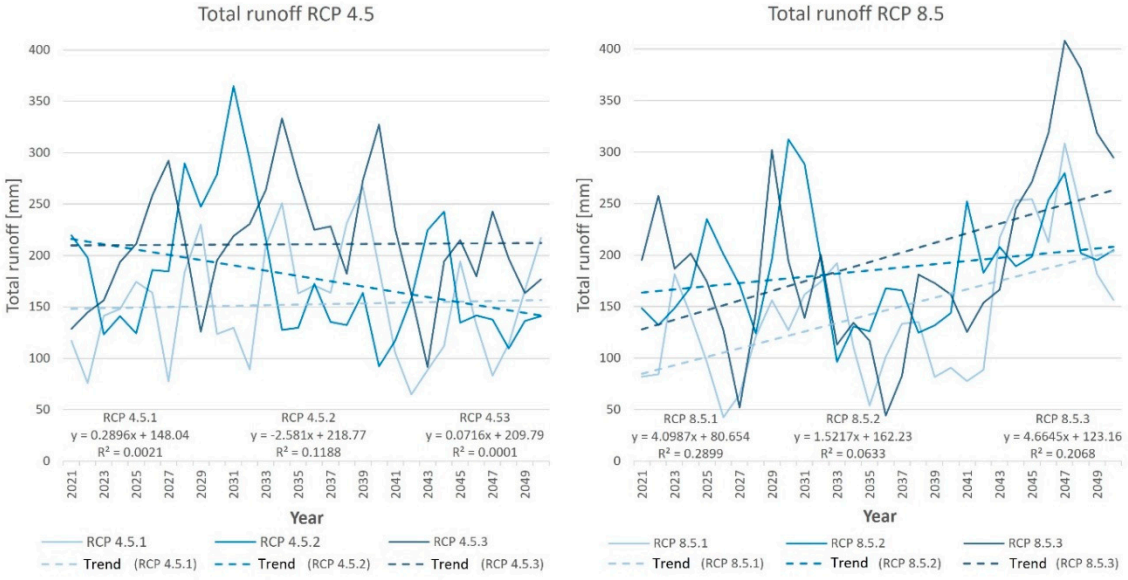

Figure 14. Average annual sum of total runoff in the Bystra River basin in the years 2021–2050 for individual climate projections in the RCP 4.5 and RCP 8.5 scenarios with trend lines (own study).

Table 10. Comparison of the average monthly total runoff for the SWAT simulation period 2010–2017 with individual projections for the RCP 4.5 and RCP 8.5 climate change scenarios for the periods 2021–2030, 2031–2040, and 2041–2050 (own study).

Climate Model	SWAT	RCP 4.5.1	RCP 4.5.2	RCP 4.5.3	RCP 8.5.1	RCP 8.5.2	RCP 8.5.3	RCP 4.5.1	RCP 4.5.2	RCP 4.5.3	RCP 8.5.1	RCP 8.5.2	RCP 8.5.3	RCP 4.5.1	RCP 4.5.2	RCP 4.5.3	RCP 8.5.1	RCP 8.5.2	RCP 8.5.3
Time Interval	**2010–2017**	**2021–2030**						**2031–2040**						**2041–2050**					
Month	**Average Monthly Total Runoff [mm]**																		
January	19	13	17	17	11	15	17	17	18	21	13	14	13	13	14	17	18	18	24
		−32%	−13%	−13%	−45%	−23%	−9%	−12%	−6%	+12%	−32%	−25%	−34%	−31%	−26%	−10%	−7%	−4%	+26%
February	18	12	16	16	9	13	15	14	16	20	11	14	11	10	13	16	16	16	22
		−32%	−7%	−10%	−47%	−24%	−12%	−22%	−10%	+11%	−39%	−20%	−36%	−45%	−28%	−9%	−8%	−8%	+27%
March	18	12	22	17	11	15	16	17	18	22	11	18	12	11	15	17	16	22	23
		−33%	+23%	−3%	−39%	−12%	−7%	−4%	+4%	+26%	−40%	+1%	−29%	−35%	−12%	−2%	−7%	+25%	+29%
April	17	11	17	15	8	14	15	13	18	20	10	14	11	10	14	16	15	20	22
		−38%	+2%	−10%	−50%	−17%	−10%	−21%	+4%	+18%	−41%	−18%	−33%	−39%	−18%	−6%	−14%	+15%	+29%
May	19	10	17	18	8	13	16	14	15	21	9	13	12	9	14	17	16	19	24
		−48%	−13%	−6%	−57%	−33%	−18%	−27%	−23%	+10%	−52%	−34%	−38%	−53%	−27%	−10%	−16%	0%	+23%
June	15	10	16	14	7	11	13	14	13	18	11	13	9	9	12	13	15	18	19
		−33%	+9%	−6%	−54%	−23%	−11%	−3%	−9%	+24%	−28%	−14%	−37%	−37%	−20%	−14%	+1%	+25%	+32%
July	16	16	17	13	8	12	12	22	16	24	9	14	9	12	11	13	15	17	20
		−3%	+3%	−18%	−53%	−30%	−28%	+32%	−2%	+47%	−45%	−17%	−45%	−30%	−34%	−19%	−9%	+3%	+19%
August	15	12	17	16	11	12	12	14	15	23	9	12	12	9	13	13	19	18	21
		−22%	+10%	+5%	−30%	−21%	−20%	−8%	-1%	+52%	−40%	−21%	−23%	−39%	−12%	−11%	+29%	+17%	+38%
September	16	13	15	19	9	12	21	17	15	24	9	11	14	11	13	15	16	18	28
		−23%	−9%	+15%	−45%	−25%	+32%	+3%	−9%	+50%	−43%	−31%	−16%	−31%	−19%	−7%	−2%	+14%	+70%
October	16	12	14	15	9	13	14	15	14	20	10	11	10	11	11	14	15	16	20
		−25%	−12%	−5%	−42%	−23%	−11%	−10%	−17%	+26%	−35%	−34%	−37%	−35%	−29%	−13%	−5%	+1%	+24%
November	16	12	16	15	9	13	14	14	13	20	10	12	10	10	11	15	17	16	22
		−25%	0%	−5%	−40%	−17%	−10%	−10%	−18%	+27%	−33%	−26%	−35%	−34%	−28%	−3%	+10%	+4%	+41%
December	18	12	17	17	10	15	16	17	13	22	12	13	11	12	13	17	21	17	24
		−30%	−6%	−2%	−44%	−16%	−9%	0%	−28%	+23%	−35%	−28%	−36%	0%	−29%	−3%	+16%	−2%	+37%
Annual sum	202	143	199	192	110	158	183	186	183	256	124	157	135	128	154	185	199	217	268
		−29%	−2%	−5%	−46%	−22%	−9%	−8%	−10%	+26%	−39%	−22%	−33%	−37%	−24%	−9%	−1%	+7%	+33%

The average annual total runoff in the decade 2041–2050 for RCP 4.5 will be lower by an average of 23%, while for RCP 8.5 it will be higher by an average of 13% compared to the simulation period.

When analyzing the spatial distribution of changes in the average annual total runoff in 31 sub-catchments for the simulation period in 2010–2017 compared to the period 2041–2050 for the RCP 4.5.1 and RCP 4.5.2 projections, the average annual total runoff amount will be lower in the entire catchment area, even reaching up to 52% (Figure 15). For RCP 4.5.3, total runoff will be lower in the northwest and southeast. It will be higher in the central part. RCP 8.5.1 and RCP 8.5.2 will have runoff volumes varying depending on the catchment area. On the other hand, the projection of RCP 8.5.3 for the whole area will have the average annual total runoff higher than in the simulation period.

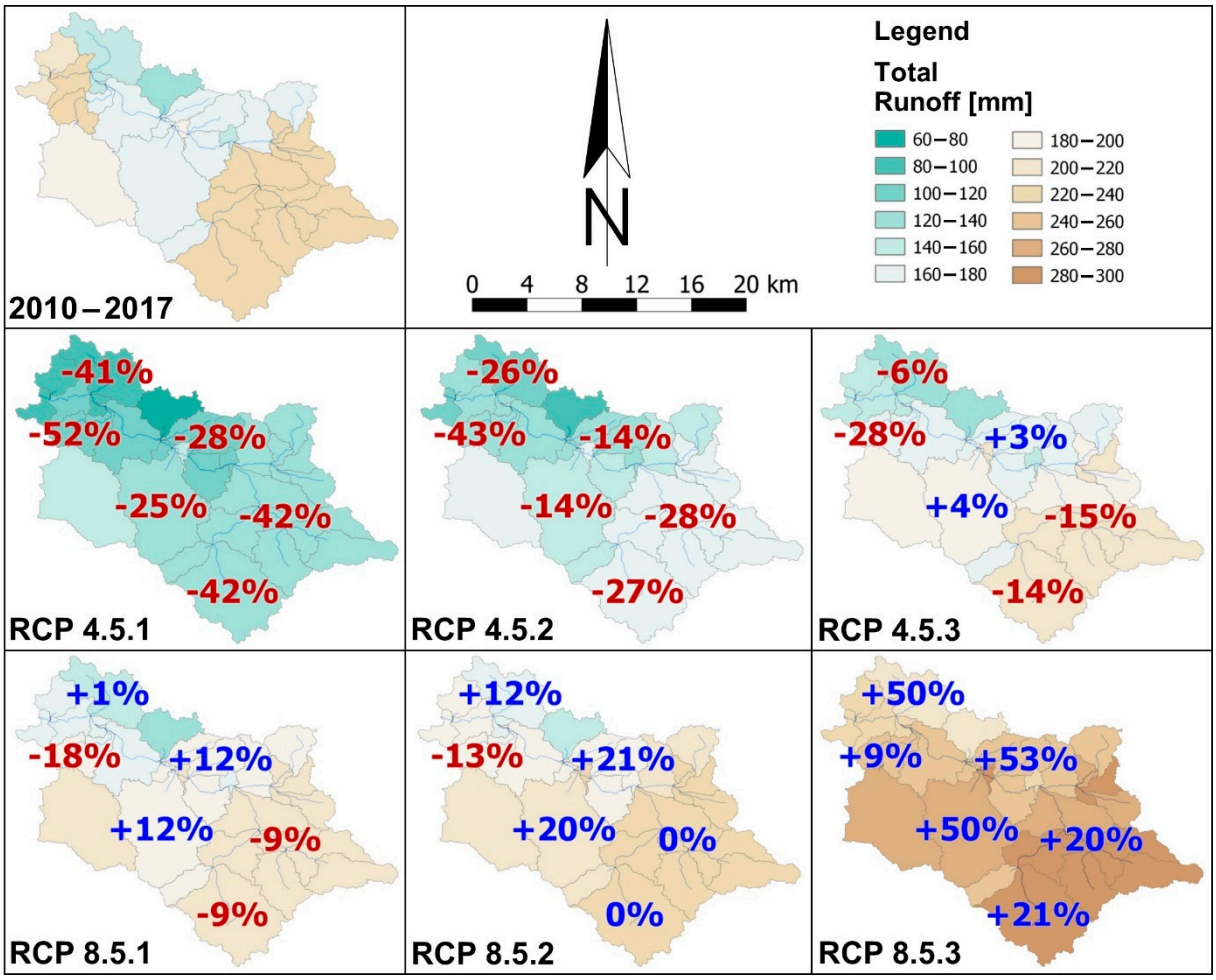

Figure 15. Comparison of the average annual sums of surface runoff in 31 sub-catchments for the SWAT simulation period 2010–2017 and 2041–2050 for individual climate projections in the RCP 4.5 and RCP 8.5 scenarios (own study).

6. Discussion

The analysis of the climate for the years 1970–2004 shows a statistically significant increase in the sum of evapotranspiration in the growing season. In the years 2021–2030, 2031–2040, and 2041–2050, an increase in potential evapotranspiration during the growing season is also shown (Table 8) [81]. Moreover, the amount of precipitation increases in winter and early spring and decreases in spring and summer. Changes in the temporal structure of precipitation may cause an increase in soil moisture in spring, which may affect areas at risk of water erosion where surface runoff should be regulated (especially

on dirt roads). This contributes to lowering the climatic water balance (i.e., increasing the precipitation deficit in relation to potential evaporation) [2,82]. Reducing the amount of precipitation, evapotranspiration, and extending the growing season caused by the temperature increase in the summer period may increase water shortages for plants [1,2].

The climate projection for Poland [82] for the years 2021–2030, 2031–2040, and 2041–2050 shows increased values of precipitation in summer (except for 2041–2050) and in autumn for the RCP 4.5 scenario compared to the period 2011–2020. However, in spring, precipitation will be lower for all decades (Table 11). Similar results were obtained for the average precipitation data in the RCP 4.5 scenario for the years 2021–2030, 2031–2040, and 2041–2050 in the SWAT model compared to the 2010–2017 simulation period. The amount of precipitation in winter is different for the SWAT and KLIMADA models for the RCP 4.5 scenario, except for the period 2031–2040, where changes in precipitation are convergent for all seasons.

The RCP 8.5 scenario for KLIMADA for the years 2021–2030, 2031–2040, and 2041–2050 shows an increased amount of precipitation for most seasons compared to the period 2011–2020. However, in the case of SWAT modeling, the years 2021–2030 and 2031–2040 show a lower amount of precipitation compared to the 2010–2017 simulation period. The exception is the period 2041–2050, where for all seasons there is an increased precipitation, similar to the RCP 8.5 scenario for KLIMADA.

The climate forecast for Poland [82] for the years 2021–2030, 2031–2040, and 2041–2050 shows increased temperatures in winter, spring, summer, and autumn (except for the period 2041–2050 for RCP 8.5). (Table 12). Similar results were obtained for averaged temperature data for winter, spring, and autumn. In summer, however, for most scenarios, temperatures will be lower in the coming decades.

In the work on a small lowland agricultural catchment in Kujawy in central Poland, the results of potential evapotranspiration, precipitation, and total runoff in 2007–2011 were presented [37,83]. The average annual potential evapotranspiration is 679 mm, the average annual precipitation is 558 mm, and the total runoff is 3.2 $L \cdot s^{-1} \cdot km^{-2}$. The above results are similar to the results of the 2010–2017 simulation in this publication, while the total runoff is higher and amounts to 6.3 $L \cdot s^{-1} \cdot km^{-2}$. This is due to the location of the tested objects. According to an academic textbook [84], the runoff value for the highlands ranges from 5 to 10 $L \cdot s^{-1} \cdot km^{-2}$. For the lowlands, it is slightly lower.

Climate change scenarios indicate a 10-fold increase in the occurrence of droughts in Poland in the coming decades [11]. According to NOAA, 2017 was the second warmest year of meteorological recording and analysis (since 1880) in the world [12]. Climate changes in the future will also affect the territory of Poland. By analyzing the climate scenarios for the years 2021–2050, it has been shown that the growing season in Poland defined by the number of days with the daily air temperature 5 °C higher in the years 2021–2050 will be longer than in the years 1971–2000 by 16 days. The predicted higher temperature in the growing season of plants will significantly accelerate their development [2]. The trend of the average annual number of days with an average temperature above 5° Celsius in the years 2020–2050 for most climate projections will be increasing, apart from the 4.5.1 projection (Figure 9).

Another publication describes, among others changes in temperature and precipitation in the near future 2021–2050 and further 2051–2100 for two hydrological models, in different climate projections for eight catchments located in Poland [85], which are similar in size to Bystra. Research shows that in the near future, warming will be ubiquitous and quite uniform spatially. In addition, there is a slight difference between the seasonal temperature increases over the period 2021–2050. In the case of precipitation, changes in the near future depend on the location of the studied catchment. For temperature and precipitation, greater differences in the results are noted for the years 2051–2100. Similar research results were obtained for the Narew River catchment for the years 2040–2069 [86].

Table 11. Comparison of the average distribution of precipitation in seasons for the SWAT simulation period 2010–2017 with individual projections for the RCP 4.5 and RCP 8.5 climate change scenarios for the periods 2021–2030, 2031–2040, and 2041–2050 (own study).

Climate Scenario	**SWAT**	**RCP 4.5**	**RCP 8.5**	**RCP 4.5**	**RCP 8.5**	**RCP 4.5**	**RCP 8.5**	**KLIMADA 2.0 RCP 4.5**				**KLIMADA 2.0 RCP 8.5**			
Time Interval	**2010–2017**	**2021–2030**		**2031–2040**		**2041–2050**		**2011–2020**	**2021–2030**	**2031–2040**	**2041–2050**	**2011–2020**	**2021–2030**	**2031–2040**	**2041–2050**
DJF	98	89	90	100	92	90	105	142	146	154	148	143	141	147	158
		−9%	−8%	+3%	−6%	−8%	+8%		+3%	+9%	+4%		−1%	+3%	+11%
MAM	156	150	142	144	134	149	176	199	182	188	185	180	180	184	192
		−4%	−8%	−7%	−14%	−4%	+13%		−9%	−6%	−7%		0%	+2%	+6%
JJA	207	230	201	243	197	194	210	218	234	234	215	222	228	224	237
		+11%	−3%	+17%	−5%	−6%	+1%		+7%	+7%	−1%		+3%	+1%	+7%
SON	135	142	148	140	130	145	169	155	162	165	165	152	163	165	176
		+5%	+10%	+3%	−4%	+7%	+25%		+4%	+6%	+6%		+7%	+8%	+16%
Annual sum	596	611	581	628	552	578	660	714	723	741	713	697	713	720	763
		+3%	−2%	+5%	−7%	−3%	+11%		+1%	+4%	0%		+2%	+3%	+10%

Table 12. Comparison of the average temperature distribution in the seasons for the SWAT simulation period 2010–2017 with individual forecasts for the RCP 4.5 and RCP 8.5 climate change scenarios for the periods 2021–2030, 2031–2040, and 2041–2050 (own study).

Climate Scenario	**SWAT**	**RCP 4.5**	**RCP 8.5**	**RCP 4.5**	**RCP 8.5**	**RCP 4.5**	**RCP 8.5**	**KLIMADA 2.0 RCP 4.5**				**KLIMADA 2.0 RCP 8.5**			
Time Interval	**2010–2017**	**2021–2030**		**2031–2040**		**2041–2050**		**2011–2020**	**2021–2030**	**2031–2040**	**2041–2050**	**2011–2020**	**2021–2030**	**2031–2040**	**2041–2050**
DJF	−1.1	−0.6	−1.1	−0.4	0.5	−0.2	0.5	−0.8	−0.7	0.4	0.1	−0.4	−0.8	0.0	0.1
		+0.6	+0.1	+0.8	+1.7	+1.0	+1.6		+0.1	+1.2	+0.9		−0.4	+0.4	+0.5
MAM	9.4	9.3	9.6	10.6	10.3	9.7	10.1	8.5	8.5	9.0	8.9	8.7	8.7	9.2	9.5
		0.0	+0.3	+1.2	+1.0	+0.3	+0.7		+0.0	+0.5	+0.4		0.0	+0.5	+0.7
JJA	19.3	18.9	18.9	19.2	19.7	19.4	19.4	18.5	18.6	18.9	19.4	18.8	18.7	19.1	19.3
		−0.4	−0.4	−0.1	+0.3	+0.1	0.0		+0.2	+0.5	+0.9		−0.1	+0.3	+0.5
SON	9.4	9.0	9.5	9.3	10.1	9.5	10.0	9.4	9.5	9.8	9.8	9.5	9.4	10.0	10.3
		−0.3	+0.1	0.0	+0.7	+0.2	+0.7		+0.1	+0.4	+0.4		−0.1	+0.4	+0.7
Annual avearge	9.2	9.2	9.2	9.7	10.1	9.6	10.0	8.9	9.0	9.5	9.5	9.2	9.0	9.6	9.8
		−0.1	0.0	+0.4	+0.9	+0.4	+0.8		+0.1	+0.6	+0.6		−0.2	+0.4	+0.6

Agriculture is strongly related to the prevailing climatic conditions but also has a large impact on them. The risk of an increase in the frequency of unfavorable climatic conditions in agriculture may result in yield variability from year to year. Water shortages during the growing season provided for in climate change scenarios will become more frequent and more severe. Other threats will include: droughts, heavy precipitation, erosion [87], floods, landslides, and strong winds [7]. The decreased precipitation from March to May is shown for most SWAT model projections for 2021–2030, 2031–2040, and 2041–2050 compared to the 2010–2017 simulation period. Increased actual evapotranspiration for the growing season may also contribute to unfavorable phenomena related to plant growth. Total runoff can also disrupt plant growth, both in terms of deficiency (e.g., RCP 4.5.1, RCP 4.5.2, RCP 4.5.3 for 2041–2050) and excess (e.g., RCP 8.5.2, RCP 8.5. 3 for the years 2041–2050).

The changes in the water balance of the Bystra River catchment in the years 2041–2050 were compared to the "Horizon 2050" variant, prepared for the Reda river catchment in the north of Poland, the waters of which flow into the Puck Bay [88]. The average monthly sums of precipitation in the "Horizon 2050" variant will be higher for the following months: February, March, April, July, September, and December compared to the calibration and validation period 1998–2006. On the other hand, the decline will cover May and November. The average monthly sums of precipitation in the remaining months will not change significantly as compared to the simulation results in the "zero" variant. The average monthly increase in precipitation in the Bystra basin in 2041–2050 will be higher in March, August, September, and November for most climate forecasts. The average monthly fall in precipitation will cover May, July and October compared to 2010–2017.

In the publication concerning the Reda catchment area, the total runoff was also analyzed. In the perspective of "Horizon 2050" compared to the calibration and validation period 1998–2006, there was an increase in total runoff for all months. Similar results were obtained for the RCP 8.5.2 and RCP 8.5.3 climate projections for the years 2041–2050, where the total runoff increased for most months, compared to the 2010–2017 simulation period.

Evapotranspiration for the Reda River catchment area in "Horizon 2050" will be higher compared to the zero variant. The increase in evapotranspiration will also occur in the years 2041–2050 compared to 2010–2017 for the Bystra River basin.

Differences between future climate changes in the Reda River basin and in the Bystra River basin may result from the location of both catchments, the calibration and validation period (for Reda it is 1998–2006; for Bystra it is 2010–2017), the climate of a given region, and prepared projections of predicted climate changes.

The publication on hydrological modeling of the Parseta River catchment area calibrated and validated the Parseta catchment area (area 2866 km^2) and two smaller catchments (area 1224 km^2 and 899 km^2) located in the Parseta catchment area [89]. The analysis of the obtained statistical coefficients (R^2, NSE) shows that the smaller the catchment supply area, the worse these coefficients were. The observed relationship between the catchment area and the applied R^2 and NSE statistics was also analyzed in other studies [90,91].

An analysis of the publication on the impact of climate change on the water resources of three Ukrainian catchments in 2040–2071 was also carried out, using the SWIM model [92]. One of the studied catchments is the Bug [93]. The research showed an increase in precipitation in 2040–2071, their seasonal variation for climate scenarios and an increase in temperature for most climate change scenarios, which is also confirmed in this article.

Similar results regarding the increase in precipitation, variation in seasonal precipitation and temperature for the climate change scenarios for the years 2071–2100 were obtained in studies of three catchments in Estonia using the SWAT model [94].

The discrepancies in the results are probably due to the higher resolution IUNG-PIB soil map (1:25,000) and the vectorized land use map used. When preparing the soil data, it was also taken into account that the available water capacity and wilting point values were appropriate for the soils of the Bystra catchment area. These values were obtained for the study titled "Assessment of Water Retention in Soil and the Risk of Drought Based on the Water Balance for the Area of the Lower Silesia" Voivodship", developed in 2013 by the

employees of the Department of Soil Science, Erosion, and Land Protection IUNG-PIB in Pulawy [20].

7. Conclusions

All climate change projections for the RCP 4.5 and RCP 8.5 scenarios show a trend of an increase in temperature.

The temperature for the coming decades will be higher for winter, spring, and autumn compared to the simulation years 2010–2017. In summer, however, temperatures will be lower in most projections in the coming decades.

The number of days with an average temperature above 5 °C will be higher for all projections (except for the RCP 4.5.1 projection).

On the other hand, the trend of the average annual number of days without rainfall for the RCP 4.5 scenario for all projections and for the RCP 8.5.2 and RCP 8.5.3 projections will increase slightly in the coming decades. For RCP 8.5.1, the trend will be downward. In the coming decades, most climate scenarios are projected to have less precipitation in spring and more in fall compared to simulation years 2010–2017. The remaining seasons show mixed results. The trend line of the average annual sum of potential evapotranspiration in the RCP 4.5.1 and RCP 8.5.2 projections will decrease in the next decades. However, in the case of RCP 4.5.2, RCP 4.5.3, RCP 8.5.1 and RCP 8.5.3 projections, the potential evapotranspiration trend line will increase. I The trend line of the average annual total actual evapotranspiration in the projections of RCP 4.5.2, RCP 8.5.3 will slightly change in the next decades. However, in the case of the RCP 4.5.1 projection, the actual evapotranspiration will decrease. For RCP 4.5.3, RCP 8.5.1 and RCP 8.5.3, the trend will be upward. In most climate projections, the monthly mean sums of actual evapotranspiration and potential evapotranspiration will be higher compared to the simulation period of the 2010–2017 model. The exception is the month of June, where actual evapotranspiration in most climate projections is lower compared to the years 2010–2017.

The total runoff will be higher for the RCP 4.5.3 (2031–2040) and RCP 8.5.2, RCP 8.5.3 (2041–2050) projections compared to the 2010–2017 simulation period. For the remaining projections, total runoff will be lower in the coming decades. The size of the total runoff depends on, e.g., climate and anthropogenic changes [88]. The higher total runoff may be due to increased precipitation and lower evapotranspiration in 2041–2050.

All of the above changes in the individual components of the water balance may have an adverse effect on plant vegetation in the 2021–2050 period. The trend of temperature increase and the variable amount of precipitation in individual months may lead to long-term climate changes as well as an increased number of extreme phenomena. Increased average monthly sum of evapotranspiration as well as changes in monthly sums of total runoff may disturb the vegetation of plants grown in the studied region at every stage of its growth, from sowing to harvesting. Probable increase in water deficits in the middle of growing season will foster substantial share of farms to adapt irrigation, which will grow in area compared to Poland's current share of irrigated fields.

Author Contributions: Conceptualization, D.B. and R.W.; methodology, D.B. and R.W.; software, D.B.; validation, D.B., R.W., J.K. and A.N.; formal analysis, B.J. and E.N.; investigation, D.B.; resources, D.B.; data curation, J.K. and A.K.-B.; writing—original draft preparation, D.B.; writing—review and editing, A.N., J.K. and A.K.-B.; visualization, D.B.; supervision, R.W.; project administration, R.W.; funding acquisition, R.W. All authors have read and agreed to the published version of the manuscript.

Funding: Research and ACP was funded by Polish Ministry of Agriculture and Rural Development, DC2.0/2021 Programme.

Institutional Review Board Statement: Not applicable.

Informed Consent Statement: Not applicable.

Data Availability Statement: Not applicable.

Conflicts of Interest: The authors declare no conflict of interest.

References

1. Kozyra, J.; Żyłowska, K.; Nieróbca, A.; Matyka, M.; Smagacz, J.; Jadczyszyn, T.; Wawer, R. *Zmiany Klimatu a Rolnictwo w Polsce Ocena Zagrożeń i Sposoby Adaptacji*; Fundacja Na Rzecz Zrównoważonego Rozwoju: Warsaw, Poland, 2019; p. 59. Available online: https://www.worldcat.org/title/zmiany-klimatu-a-rolnictwo-w-polsce-ocena-zagroe-i-sposoby-adaptacji/oclc/1150352150#borrow (accessed on 3 March 2018).
2. KLIMADA. Adaptacja Do Zmian Klimatu. 2013. Available online: http://klimada.mos.gov.pl/?p=150 (accessed on 22 December 2018).
3. Badora, D.; Wawer, R.; Nieróbca, A.; Król-Badziak, A.; Kozyra, J.; Jurga, B. Hydrological Water Balance in Vistula River Catchment in Climate Projections 2020–2050 for RCP 4.5 and RCP 8.5 Climate Change Scenarios. *Water* 2022, *in press*.
4. Jacob, D.; Kotova, L.; Teichmann, C.; Sobolowski, S.P.; Vautard, R.; Donnelly, C.; Koutroulis, A.G.; Grillakis, M.G.; Tsanis, I.K.; Damm, A.; et al. Climate Impacts in Europe Under +1.5 °C Global W'rming. *Earth's Future.* **2018**, *6*, 264–285. [CrossRef]
5. Kovats, R.S.; Valentini, R.; Bouwer, L.M.; Georgopoulou, E.; Jacob, D.; Martin, E.; Rounsevell, M.; Soussana, J.-F. Europe. In *Climate Change 2014: Impacts, Adaptation, and Vulnerability. Part B: Regional Aspects. Contribution of Working Group II to the Fifth Assessment Report of the Intergovernmental Panel on Climate Change*; Barros, V.R., Field, C.B., Dokken, D.J., Mastrandrea, M.D., Mach, K.J., Bilir, T.E., Chatterjee, M., Ebi, K.L., Estrada, Y.O., Genova, R.C., et al., Eds.; Cambridge University Press: Cambridge, UK; New York, NY, USA, 2014; pp. 1267–1326.
6. Doroszewski, A.; Jadczyszyn, J.; Kozyra, J.; Pudełko, R.; Stuczyński, T.; Mizak, K.; Łopatka, A.; Koza, P.; Górski, T.; Wróblewska, E. Podstawy systemu monitoringu suszy rolniczej. *Woda-Środowisko-Obsz. Wiej.* **2012**, *12*, 78–91.
7. Kundzewicz, Z.; Kozyra, J. Ograniczenie wpływu zagrożeń klimatycznych w odniesieniu do rolnictwa i obszarów wiejskich. *Pol. J. Agron.* **2011**, *7*, 68–81.
8. Kundzewicz, Z. Zmiany klimatu, ich przyczyny i skutki–możliwości przeciwdziałania i adaptacji. *Studia BAS.* **2012**, *1*, 9–30.
9. Zeder, J.; Fischer, E.M. Observed extreme precipitation trends and scaling in Central Europe. *Weather Clim. Extrem.* **2020**, *29*, 100266. [CrossRef]
10. IPCC. *Climate Change 2007: Synthesis Report. Contribution of Working Groups I, II and III to the Fourth Assessment Report of the Intergovernmental Panel on Climate Change*; Core Writing Team, Pachauri, R.K., Reisinger, A., Eds.; IPCC: Geneva, Switzerland, 2007; p. 104.
11. Parry, M.L.; Canziani, O.F.; Palukitof, J.P.; van der Linden, P.J.; Hanson, C.E. *Contribution of Working Group II to the Fourth Assessment Report of the Intergovernmental Panel on Climate Change*; Cambridge University Press: Cambridge, UK; New York, NY, USA, 2007. Available online: https://www.ipcc.ch/publications_and_data/ar4/wg2/en/contents.html (accessed on 12 December 2015).
12. NOAA. National Oceanic and Atmospheric Administration, Global Summary–Informat–on-January 2018. Available online: https://www.ncdc.noaa.gov/sotc/global/201713 (accessed on 3 March 2018).
13. Ministerstwo Środowiska (Ministry of the Environment), Strategiczny Plan Adaptacji dla Sektorów i Obszarów Wrażliwych na Zmiany Klimatu do Roku 2020 z Perspektywą do Roku 2030. Dokument Został Opracowany Przez Ministerstwo Środowiska na Podstawie Analiz Wykonanych Przez Instytut Ochrony Środowiska—Państwowy Instytut Badawczy w Ramach Projektu: "Opracowanie i Wdrożenie Strategicznego Planu Adaptacji dla Sektorów i Obszarów Wrażliwych na Zmiany Klimatu—KLIMADA", Realizowanego na Zlecenie MŚ w Latach 2011–2013 ze Środków Narodowego Funduszu Ochrony Środowiska i Gospodarki Wodnej, Warsaw, Poland. 2013. Available online: https://bip.mos.gov.pl/fileadmin/user_upload/bip/strategie_plany_programy/Strategiczny_plan_adaptacji_2020.pdf (accessed on 15 May 2019).
14. Doroszewski, A.; Jóźwicki, T.; Wróblewska, E.; Kozyra, J. *Susza Rolnicza w Polsce w Latach 1961–2010*; Wyd, IUNG-PIB: Pulawy, Poland, 2014; p. 144. ISBN 978-83-7562-171-6.
15. Doroszewski, A. Lecture: Susza Rolnicza w Polsce w 2015 Roku; Warsaw, Poland. 2016. Available online: https://docplayer.pl/31410328-Susza-rolnicza-w-polsce-w-2015-roku-andrzej-doroszewski.html (accessed on 12 April 2020).
16. Huo, R.; Li, L.; Chen, H.; Xu, C.; Chen, J.; Guo, S. Extreme Precipitation Changes in Europe from the Last Millennium to the End of the Twenty-First Century. *J. Clim.* **2021**, *34*, 567–588. Available online: https://journals.ametsoc.org/view/journals/clim/34/2/JCLI-D-19-0879.1.xml (accessed on 15 December 2021). [CrossRef]
17. Mishra, V.; Cherkauer, K.A.; Shukla, S. Assessment of drought due to *h*istoric *c*limate variability and *p*rojected future climate change in the Midwestern United States. *J. Hydrometeorol.* **2010**, *11*, 46–68. Available online: https://journals.ametsoc.org/view/journals/hydr/11/1/2009jhm1156_1.xml (accessed on 3 February 2022). [CrossRef]
18. Piniewski, M.; Szcześniak, M.; Kundzewicz, Z.W.; Mezghani, A.; Hov, Ø. Changes in low and high flows in the Vistula and the Odra basins: Model projections in the European-scale context. *Hydrol. Process.* **2017**, *31*, 2210–2225. [CrossRef]
19. Brzóska, B.; Jaczewski, A. Przyszłe zmiany wybranych wskaźników klimatycznych dla Polski na podstawie wyników dynamicznego downscalingu, zeszyt. *Pr. Geogr.* **2017**, *149*, 7–14. [CrossRef]
20. IUNG-PIB. *Ocena Retencji Wody w Glebie i Zagrożenia Suszą w Oparciu o Bilans Wodny dla Obszaru Województwa Dolnośląskiego*; Zakład Gleboznawstwa Erozji i Ochrony Gruntów, IUNG-PIB: Pulawy, Poland, 2013.

21. Jurga, B.; Wawer, R.; Kęsik, K. Zlewnia rzeki Bystrej jako przykład wyżynnej zlewni rolniczej o wysokich zdolnościach buforowych względem fosforu- studium przypadku. In *Rolnictwo XXI Wieku–Problemy i Wyzwania*; Łuczyckiej, D., Ed.; Idea Knowledge Future: Wrocław, Poland, 2018; pp. 143–154. ISBN 978-83-945311-9-5.
22. Chałubińska, A.; Wilgat, T. Podział Fizjograficzny Województwa Lubelskiego. In *Przewodnik V Ogólnopolskiego Zjazdu Polskiego Towarzystwa Geograficznego*; Oddział lubelski PTG: Lublin, Poland, 1954; pp. 3–44.
23. Jahn, A. *Wyżyna Lubelska; Rzeźba i Czwartorzęd*; Prace Geograficzne Instytutu Geograficznego, Nr 7, IGiPAN, PWN: Warszawa, Poland, 1956.
24. Sadurska, E. *Charakterystyka Fizycznogeograficzna Dorzecza Bystrej. Z. 29*; IUNG: Puławy, Poland, 1980.
25. Ziemnicki, S.; Pałys, S. Erozja wodna w zlewni rzeki Bystrej. *Zesz. Probl. Postępów Nauk Rol.* **1977**, *193*, 44–71.
26. Wawer, R.; Nowocień, E.; Podolski, B.; Capała, M. Ocena zagrożenia erozją wodną i powierzchniową zlewni rzeki Bystrej z wykorzystaniem modelowania przestrzennego. *Przegląd Naukowy SGGW Inżynieria i Kształtowanie Środowiska.* **2008**, *XVII*, 20–28.
27. SMGP. Szczegółowa Mapa Geologiczna Polski, Arkusz 747–Nałęczów (M-34-33-A). 2006. Available online: http://bazadata.pgi.gov.pl/data/smgp/arkusze_skany/smgp0747.jpg (accessed on 6 September 2018).
28. Wawer, R.; Nowocień, E.; Kozyra, J. Hydrologia i Denudacja w zlewni rzeki Bystrej. In Proceedings of the Konferencja Problemy Gospodarowania Zasobami Środowiska w Dolinach Rzecznych, Wrocław, Poland, 27–29 May 2015.
29. Maruszczak, H. Definicja i klasyfikacja lessów oraz utworów lessopodobnych. *Przegląd Geol.* **2000**, *48*, 580–586.
30. Kalarus, K. *Wpływ Materiału Macierzystego na Właściwości Gleb Wykształconych na Lessie*; Uniwersytet Jagieloński, Wydział Biologii i Nauk o Ziemi: Kraków, Poland, 2009.
31. Piest, R.F.; Ziemnicki, S. Comparative erosion rates of loeass soils in Poland and Iowa. *Trans. ASAE.* **1979**, *22*, 822–827. [CrossRef]
32. Arnold, J.G.; Kiniry, J.R.; Srinivasan, R.; Williams, J.R.; Haney, E.B.; Neitsch, S.L. Soil and Water Assessment Tool Theoretical Documentation. Version 2012. Available online: https://swat.tamu.edu/media/69296/swat-io-documentation-2012.pdf (accessed on 15 December 2021).
33. QGIS. Quantum GIS 3.10.13 Coruna. 2020. Available online: http://www.qgis.org/pl/site/index.html (accessed on 3 March 2020).
34. Winchell, M.; Srinivasan, R. *SWAT Editor for SWAT2012—Documentation*; Blackland Research Center: Temple, TX, USA, 2012; pp. 1–14.
35. USDA. United States Department of Agriculture. 1996. Available online: https://www.usda.gov/ (accessed on 1 December 2020).
36. Arnold, J.G.; Srinivasan, R.; Muttiah, R.; Williams, J. Large area hydrologic modeling and assessment. P. I: Model development. *J. Am. Water Resour. Assoc.* **1998**, *34*, 73–89. [CrossRef]
37. Miatkowski, Z.; Smarzyńska, K. Calibration and validation of SWAT model for estimating water balance and nitrogen losses in a small agricultural watershed in central Poland. *J. Water Land Dev.* **2016**, 31–47. [CrossRef]
38. Neitsch, S.L.; Arnold, J.G.; Kiniry, J.R.; Williams, J.R. Soil and Water Assessment Tool. Theoretical Documentation Version. 2005. Available online: http://swatmodel.tamu.edu/media/1292/swat2005theory.pdf (accessed on 2 January 2020).
39. Bajkiewicz-Grabowska, E.; Mikulski, Z. *Hydrologia Ogólna*; Wojtala, K., Ed.; Polish Scientific Publishers PWN: Warszaw, Poland, 2010; ISBN 978-83-01-14579-8.
40. Neitsch, S.I.; Arnold, J.G.; Kiniry, J.R.; Williams, J.R. *Soil and Water Assessment Tool Theoretical Documentation. Version 2009*; Texas Water Resources Institute: College Station, TX, USA, 2011.
41. Ulańczyk, R. Materiały informacyjne (QSWAT). In Proceedings of the Szkolenie Dotyczące Modelu SWAT (Soil and Water Assessment Tool) Oraz Interfejsu QSWAT, Sosnowiec, Poland, 14–16 May 2018.
42. Abbaspour, K.C. *SWAT-CUP 2012: SWAT Calibration and Uncertainty Programs—A User Manual*; Eawag: Dübendorf, Switzerland, 2012.
43. Abbaspour, K.C.; Vejdani, M.; Haghighat, S. SWAT-CUP calibration and uncertainty programs for SWAT. In Proceedings of the International Congress on Modelling and Simulation (MODSIM'07), Christchurch, New Zealand, 10–13 December 2007; Oxley, L., Kulasiri, D., Eds.; Modelling and Simulation Society of Australia and New Zealand: Melbourne, Australia, 2007; pp. 1603–1609.
44. Abbaspour, K.C.; Yang, J.; Maximov, I.; Siber, R.; Bogner, K.; Mieleitner, J.; Zobrist, J.; Srinivasan, R. Modelling hydrology and water quality in the prealpine/alpine Thur watershed using SWAT. *J. Hydrol.* **2007**, *333*, 413–430. [CrossRef]
45. Bilondi, M.P.; Abbaspour, K.C.; Ghahraman, B. Application of three different calibration-uncertainty analysis methods in a semi-distributed rainfall-runoff model application. *Middle-East J. Sci. Res.* **2013**, *15*, 1255–1263.
46. Yang, W.; Andréasson, J.; Phil Graham, L.; Olsson, J.; Rosberg, J.; Wetterhall, F. Distribution-based scaling to improve usability of regional climate model projections for hydrological climate change impacts studies. *Hydrol. Res.* **2010**, *41*, 211–229. [CrossRef]
47. CODGiK. Centralny Ośrodek Dokumentacji Geodezyjnej I Kartograficznej. 2013. Available online: http://www.codgik.gov.pl/ (accessed on 2 February 2017).
48. MPHP. Komputerowa Mapa Podziału Hydrograficznego Polski. 2017. Available online: https://danepubliczne.gov.pl/dataset?q=zlewnia&sort=metadata_modified+desc (accessed on 4 June 2018).
49. KPOŚK. Krajowy Program Oczyszczania Ścieków Komunalnych. 2017. Available online: https://www.kzgw.gov.pl/index.php/pl/materialy-informacyjne/programy/krajowy-program-oczyszczania-sciekow-komunalnych (accessed on 3 March 2020).
50. Jadczyszyn, J.; Smreczak, B. Mapa glebowo-rolnicza w skali 1:25 000 i jej wykorzystanie na potrzeby współczesnego rolnictwa. *Studia i Reporty IUNG PI.* **2017**, *51*, 9–27. [CrossRef]
51. IUNG-PIB. *Igital s–Il-Agricultural Maps 1:25,000 and 1:100,000*; IUNG-PIB: Pulawy, Poland, 2010.

52. CLC. CORIN–Land Cover-CLC. Główny Inspektorat Ochrony Środowiska. 2018. Available online: http://clc.gios.gov.pl/index.php/clc-2018/o-clc2018 (accessed on 25 June 2018).
53. Geoportal. Instytucja Odpowiedzialna: Główny Urząd Geodezji i Kartografii. 2020. Available online: www.geoportal.gov.pl;https://mapy.geoportal.gov.pl/wss/service/PZGIK/ORTO/WMS/HighResolution (accessed on 5 March 2020).
54. OSM. Open Street Map. 2018. Available online: http://download.geofabrikolandrolandland.html (accessed on 6 September 2019).
55. IMGW. Instytut Meteorologii i Gospodarki Wodnej PIB. 2019. Available online: http://danepubliczne.imgw.pl/data/dane_pomiarowo_obserwacyjne/ (accessed on 3 March 2019).
56. Wawer, R.; Nowocień, E.; Podolski, B. Actual water erosion risk in Poland based upon Corine Land Cover 2006. *EJPAU.* **2010**, *13*, 13. Available online: http://www.ejpau.media.pl/volume13/issue2/art-13.html (accessed on 10 December 2021).
57. Józefaciuk, C.Z.; Józefaciuk, A.; Nowocień, E.; Wawer, R. *Przeciwerozyjne Zagospodarowanie Zlewni Wyżynnej Potoku Grodarz z Uwzględnieniem Ograniczania Występowania Powodzi*; IUNG: Pulawy, Poland, 2002; Volume 4, p. 65. ISBN 83-88031-84-8.
58. Nowocień, E. Wybrane zagadnienia erozji gleb w Polsce–Ocena zagrożenia gleb erozją. *Studia i Raporty IUNG-PIB.* **2008**, *10*, 9–29. [CrossRef]
59. Markowski, K. *Rolnictwo w Województwie Lubelskim w 2019 r*; Urząd Statystyczny w Lublinie: Lublin, Poland, 2020; ISSN 2080-0517.
60. Lasy Regionu (The Forests of the Region), Regionalna Dyrekcja Lasów Państwowych w Lublinie. Available online: https://www.lublin.lasy.gov.pl/lasy-regionu#.yg89jegzzaq (accessed on 5 July 2019).
61. Essenfelder, A.H. SWAT Weather Database—A Quick Guide. 2018. Available online: https://www.researchgate.net/publication/330221011_SWAT_Weather_Database_A_Quick_Guide (accessed on 3 March 2019).
62. Abbaspour, K.C.; Rouholahnejad, E.; Vaghefi, S.; Srinvasan, R.; Yang, H.; Kløve, B. A continental-scale hydrology and water quality model for Europe: Calibration and uncertainty of a high-resolution large-scale SWAT model. *J. Hydrol.* **2015**, *524*, 733–752. [CrossRef]
63. Abbaspour, K.C.; Vaghefi, S.A.; Srinivasan, R.A. Guideline for successful calibration and uncertainty analysis for soil and water assessment: A review of papers from the 2016 International SWAT Conference. *Water* **2018**, *10*, 6. [CrossRef]
64. Arnold, J.G.; Moriasi, D.N.; Gassman, P.W.; Abbaspour, K.C.; White, M.J.; Srinivasan, R.; Santhi, C.; Harmel, R.D.; Griensven, A.; Van Liew, M.W.; et al. Swat: Model use, calibration, and validation. *Trans. ASABE.* **2012**, *55*, 1491–1508. [CrossRef]
65. Kouchi, D.M.; Esmaili, K.; Faridhosseini, A.; Sanaeinejad, S.H.; Khalili, D.; Abbaspour, K.C. Sensitivity of Calibrated Parameters and Water Resource Estimates on Different Objective Functions and Optimization Algorithms, MDPI. *Water* **2017**, *9*, 384. [CrossRef]
66. Abbaspour, K.C. SWAT-CUP Tutorial (2): Introduction to SWAT-CUP program, Parameter Estimator (SPE). 2020. Available online: https://www.youtube.com/watch?v=nNsDPhOI7cc&ab_channel=2w2e,2w2eGmbH (accessed on 15 December 2021).
67. Gao, X.; Chen, X.; Biggs, T.; Yao, H. Separating Wet and Dry Years to Improve Calibration of SWAT in Barrett Watershed, Southern California, MDPI. *Water.* **2018**, *10*, 274. [CrossRef]
68. ADMS. Agricultural Drought Monitoring System. 2013. Available online: https://susza.iung.pulawy.pl/system/ (accessed on 10 February 2022).
69. Hennemuth, T.I.; Jacob, D.; Keup-Thiel, E. Guidance for EURO-CORDEX Climate Projections Data Use. Version1 0-201708. 2017. Available online: https://www.euro-cordex.net/imperia/md/content/csc/cordex/euro-cordex-guidelines-version1.0-2017.08.pdf (accessed on 13 January 2020).
70. Jacob, D.; Petersen, J.; Eggert, B.; Alias, A.; Christensen, O.B.; Bouwer, L.M.; Braun, A.; Colette, A.; Déqué, M.; Georgievski, G. EURO-CORDEX: New high-resolution climate change projections for European impact research. *Reg. Environ. Chang.* **2014**, *14*, 563–578. [CrossRef]
71. Moss, R.H.; Edmonds, J.A.; Hibbard, K.A.; Manning, M.R.; Rose, S.K.; Van Vuuren, D.P.; Carter, T.R.; Emori, S.; Kainuma, M.; Kram, T. The next generation of scenarios for climate change research and assessment. *Nature.* **2010**, *463*, 747–756. [CrossRef]
72. Thomson, A.M.; Calvin, K.V.; Smith, S.J.; Kyle, G.P.; Volke, A.; Patel, P.; Delgado-Arias, S.; Bond-Lamberty, B.; Wise, M.A.; Clarke, L.E. RCP4. 5: A pathway for stabilization of radiative forcing by 2100. *Clim. Chang.* **2011**, *109*, 77–94. [CrossRef]
73. Yang, J.; Reichert, P.; Abbaspour, K.C.; Xia, J.; Yang, H. Comparing uncertainty analysis techniques for a SWAT application to the Chaohe Basin in China. *J. Hydrol.* **2008**, *358*, 1–23. [CrossRef]
74. Landelius, T.; Dahlgren, P.; Gollvik, S.; Jansson, A.; Olsson, E. A high-resolution regional reanalysis for Europe. Part 2: 2D analysis of surface temperature, precipitation and wind. *Q. J. R. Meteorol. Soc.* **2016**, *142*, 2132–2142. [CrossRef]
75. Schulzweida, U.; Kornblueh, L.; Quast, R. CDO 'ser's guide. *Clim. Data Oper. Version* **2006**, *1*, 205–209.
76. Kundzewicz, Z.W.; Piniewski, M.; Mezghani, A.; Okruszko, T.; Pińskwar, I.; Kardel, I.; Hov, Ø.; Szcześniak, M.; Szwed, M.; Benestad, R.E.; et al. Assessment of climate change and associated impact on selected sectors in Poland. *Acta Geophys.* **2018**, *66*, 1509–1523. [CrossRef]
77. Czernecki, B.; Ptak, M. The impact of global warming on lake surface water temperature in Poland–the application of empirical–statistical downscaling, 1971–2100. *J. Limnol.* **2018**, *77*, 330–348. [CrossRef]
78. IPPC. Intergovernmental Panel on Climate Change. 1998. Available online: https://www.ipcc.ch/ (accessed on 7 May 2020).
79. PIK. Potsdam Institute for Climate Impact Research. 2012. Available online: http://www.pik-potsdam.de/~{}mmalte/rcps/ (accessed on 5 August 2021).

80. Meinshausen, M.; Smith, S.J.; Calvin, K.V.; Daniel, J.S.; Kainuma, M.L.T.; Lamarque, J.-F.; Matsumoto, K.; Montzka, S.A.; Raper, S.C.B.; Riahi, K.; et al. The RCP Greenhouse Gas Concentrations and their Extension from 1765 to 2300. *Clim. Chang.* **2011**, *109*, 213–241. [CrossRef]
81. Łabędzki, L.; Bąk, B.; Kanecka-Geszke, E. Wielkość i zmienność ewapotranspirację wskaźnikowej według Penmana-Monteitha w okresie wegetacyjnym w latach 1970–2004 w wybranych rejonach Polski, Instytut Technologiczno-Przyrodniczy, Kujawsko-Pomorski Ośrodek Badawczy w Bydgoszczy. *WODA-Środowisko-OBSZARY WIEJSKIE* **2012**, *2*, 159–170.
82. KLIMADA 2.0. KLIMADA 2.0–Baza Wiedzy o Zmianach Klimatu, Scenariusze Zmian Klimatu. 2019. Available online: https://www.itp.edu.pl/old/wydawnictwo/woda/zeszyt_38_2012/artykuly/Labedzki%20in.pdf (accessed on 2 February 2022).
83. Miatkowski, Z.; Smarzyńska, K. Surface water resources of small agricultural watershed in the Kujawy region, central Poland. *J. Water Land Dev.* **2017**, *33*, 131–140. [CrossRef]
84. Dynowska, I.; Pociask-Karteczka, J. *Obieg Wody [w:] Starkel L. (Red.), Geografia Polski*; Środowisko Przyrodnicze, Wyd, Nauk, PWN: Warszawa, Poland, 1999.
85. Piniewski, M.; Meresa, H.K.; Romanowicz, R. What can we learn from the projections of changes of flow patterns? Results from Polish case studies. *Acta Geophys.* **2017**, *65*, 809–827. [CrossRef]
86. Piniewski, M. *Impacts of Natural and Anthropogenic Conditions on the Hydrological Regime of Rivers: A Narew River Basin Case Study*; Instytut Meteorologii i Gospodarki Wodnej: Warszawa, Poland, 2012.
87. Józefaciuk, A.; Nowocień, E.; Wawer, R. *Erozja Gleb w Polsce–Skutki Środowiskowe i Gospodarcze, Działania Zaradcze*; nr 44; Monografie i Rozprawy Naukowe IUNG-PIB: Pulawy, Poland, 2014; p. 263.
88. Marcinkowski, P.; Piniewski, M.; Kardel, I.; Giełczewski, M.; Okruszko, T. Modelling of discharge, nitrate and phosphate loads from the Reda catchment to the Puck Lagoon using SWAT. *Ann. Warsaw Univ. Life Sci. –SGGW Land Reclam.* **2013**, *45*, 125–141. [CrossRef]
89. Gudowicz, J.; Zwoliński, Z. Kształtowanie się odpływu rzecznego w dorzeczu Parsęty w świetle modelowania hydrologicznego. *Przegląd Geogr.* **2017**, *89*, 45–66. [CrossRef]
90. Piniewski, M.; Okruszko, T. *Multi-Site Calibration and Validation of the Hydrological Component of SWAT in a Large Lowland Catchment, [w:] D. Świątek, T. Okruszko (Red.), Modelling of Hydrological Processes in the Narew Catchment, Geoplanet: Earth and Planetary Sciences*; Springer: Berlin, Germany, 2011; pp. 15–41.
91. Piniewski, M.; Marcinkowski, P.; Kardel, I.; Giełczewski, M.; Izydorczyk, K.; Frątczak, W. Spatial quantifi cation of non-point source pollution in a meso-scale catchment for an assessment of buffer zones effi ciency. *Water* **2015**, *7*, 1889–1920. [CrossRef]
92. Krysanova, V.; Wechsung, F.; Arnold, J.; Ragavan, S.; Williams, J. *SWIM (Soil and Water Integrated Model), User Manual*; Report Nr. 69; Potsdam Institute Climate Impact Research (PIK): Potsdam, Germany, 2000.
93. Didovets, I.; Lobanova, A.; Bronstert, A.; Snizhko, S.; Maule, C.F.; Krysanova, V. Assessment of climate change impacts on water resources in three representative Ukrainian catchments using eco-hydrological modelling. *Water* **2017**, *9*, 204. [CrossRef]
94. Tamm, O.; Luhamaa, A.; Tamm, T. Modeling future changes in the North-Estonian hydropower production by using. *Hydrol. Res.* **2016**, *47*, 835–846. [CrossRef]